NASA TECHNICAL NOTE

A THEORETICAL ANALYSIS OF AIRPLANE LONGITUDINAL STABILITY AND CONTROL AS AFFECTED BY WIND SHEAR

Windsor L. Sherman

Langley Research Center
Hampton, Va. 23665

NATIONAL AERONAUTICS AND SPACE ADMINISTRATION • WASHINGTON, D. C. • JULY 1977

Completed
21 Feb 78 5A

ERRATA

NASA Technical Note D-8496

A THEORETICAL ANALYSIS OF AIRPLANE LONGITUDINAL STABILITY AND CONTROL AS AFFECTED BY WIND SHEAR

Windsor L. Sherman
July 1977

The units for the following symbols appearing on pages 2, 3, 4, and 5 should read:

g	$m\text{-}sec^{-2}$
I_1	$kg\text{-}m^2$
I_2	$kg\text{-}m^2$
I_3	$kg\text{-}m^2$
M_q	$rad^{-1}\text{-}sec^{-1}$
$v_{w,1}, v_{w,2}, v_{w,3}$	$m\text{-}sec^{-1}$
W_i	$m\text{-}sec^{-1}$
Γ_c	rad
τ	sec
τ_E	sec
ω_p	$rad\text{-}sec^{-1}$

Page 8, table II: Delete arrow in column headed $T_{1/2}$, sec. The last entry in column headed ζ_p should be .0528.

Page 21: M = 90 909.1 kg should read m = 90 909.1 kg. The dimensions for Z_q should read $m\text{-}rad^{-1}\text{-}sec^{-1}$.

Issued January 1978

1. Report No. NASA TN D-8496	2. Government Accession No.	3. Recipient's Catalog No.
4. Title and Subtitle A THEORETICAL ANALYSIS OF AIRPLANE LONGITUDINAL STABILITY AND CONTROL AS AFFECTED BY WIND SHEAR		5. Report Date July 1977 6. Performing Organization Code
7. Author(s) Windsor L. Sherman		8. Performing Organization Report No. L-11392
9. Performing Organization Name and Address NASA Langley Research Center Hampton, VA 23665		10. Work Unit No. 505-08-26-02 11. Contract or Grant No.
12. Sponsoring Agency Name and Address National Aeronautics and Space Administration Washington, DC 20546		13. Type of Report and Period Covered Technical Note 14. Sponsoring Agency Code
15. Supplementary Notes		

16. Abstract

Wind shear, the variation of horizontal wind velocity with altitude, has been a causative factor in several airplane accidents and may have been a contributing factor in other accidents. The longitudinal equations of motion with wind shear terms were used to analyze the stability and motions of a jet transport. A positive wind shear gives a decreasing head wind or changes a head wind into a tail wind. A negative wind shear gives a decreasing tail wind or changes a tail wind into a head wind. It was found that wind shear had very little effect on the short period mode and that negative wind shear, although it affected the phugoid, did not cause stability problems. On the other hand, it was found that positive wind shear can cause the phugoid to become aperiodic and unstable. In this case, a stability boundary for the phugoid was found that is valid for most aircraft at all flight speeds. Calculations of aircraft motions confirmed the results of the stability analysis. It was found that a flight-path control automatic pilot and an airspeed control system provide good control in all types of wind shear. Appendixes give equations of motion that include the effects of downdrafts and updrafts and extend the longitudinal equations of motion for shear to six degrees of freedom.

17. Key Words (Suggested by Author(s)) Wind shear Stability Control	18. Distribution Statement Unclassified - Unlimited Subject Category 08

19. Security Classif. (of this report)	20. Security Classif. (of this page)	21. No. of Pages	22. Price*
Unclassified	Unclassified	51	$4.50

* For sale by the National Technical Information Service, Springfield, Virginia 22161

A THEORETICAL ANALYSIS OF AIRPLANE LONGITUDINAL STABILITY AND CONTROL AS AFFECTED BY WIND SHEAR

Windsor L. Sherman
Langley Research Center

SUMMARY

Wind shear, the variation of horizontal wind velocity with altitude, has been a causative factor in several airplane accidents and may have been a contributing factor in other accidents. The longitudinal equations of motion with wind shear terms were used to analyze the stability and motions of a jet transport. A positive wind shear gives a decreasing head wind or changes a head wind into a tail wind. A negative wind shear gives a decreasing tail wind or changes a tail wind into a head wind. It was found that wind shear had very little effect on the short period mode and that negative wind shear, although it affected the phugoid, did not cause stability problems. On the other hand, it was found that positive wind shear can cause the phugoid to become aperiodic and unstable. In this case, a stability boundary for the phugoid was found that is valid for most aircraft at all flight speeds. Calculations of aircraft motions confirmed the results of the stability analysis.

It was found that a flight-path control automatic pilot and an airspeed control system provide good control in all types of wind shear. Appendixes give equations of motion that include the effects of downdrafts and updrafts and extend the longitudinal equations of motion for shear to six degrees of freedom.

INTRODUCTION

Wind shear, that is, the change in the horizontal components of the wind with altitude, has been a causative agent in several airplane crashes that occurred during final approach. (See refs. 1 and 2.) In addition to these accidents which caused a loss of life of 246 persons and injuries to many more people, wind shear may be an unidentified factor in many more accidents that occur during final approach and landing. Two of these accidents, the crash of Iberia Airlines, Flight 933, on December 17, 1973, at Logan International Airport (ref. 2), and the crash of Eastern Airlines, Flight 66, at John F. Kennedy International Airport on June 24, 1975 (ref. 3), are of particular interest because the wind shear profiles for these accidents are available; thus, an analytical investigation of airplane stability and control in accident-causing wind shears is possible.

Considerable work has been done on the effects of wind shear (refs. 4 to 7), and it has concentrated on the effect on touchdown conditions. Gera (ref. 7) has formulated the longitudinal equations of motion of the airplane so that the dynamic effects of wind shear are considered. In reference 7, the

major concern was the effect on landing conditions and some stability considerations were included.

The present paper adopts Gera's formulation of the problem as a starting point for the investigation of the longitudinal stability of the airplane, and the use of automatic control systems to improve the longitudinal characteristics. The results presented are not as restrictive as would generally be supposed because the analysis of the accidents reported in references 2 and 3 indicated little or no effect on the lateral modes of motion. In addition to the work on longitudinal stability, a formulation of the six-degree-of-freedom equations of motion based on Gera's approach is given.

The airplane equations of motion used in the analysis are presented in appendix A. The airplane characteristics and flight condition are given in appendix B. Phugoid stability in wind shear is discussed in appendix C.

SYMBOLS

The SI system of units is used throughout this paper. All angles are in radians.

$\bar{c}$	mean aerodynamic chord, m
D	distance along approach path, m; or d/dt
E(D)	numerator of airplane transfer function
$\vec{F}$	force vector
F_1,F_2,F_3	forces along x_1, x_2, and x_3, N
$F_{y,1},F_{y,3}$	forces along y_1 and y_3 axes, N
g	acceleration due to gravity, m-sec^{-2}
H(D)	denominator of airplane transfer function
h	altitude, m
I_1	moment of inertia about x_1, kg-m^2
I_2	moment of inertia about x_2 and y_2, kg-m^2
I_3	moment of inertia about x_3, kg-m^2
i,j	indices, 1, 2, 3
$k,k_1,\ldots k_7$	gains
ℓ	characteristic length, m

ℓ_{ij} direction cosines

$M_q = \frac{1}{I_2} \frac{\partial M_2}{\partial \dot{\theta}}$, $rad^{-1}\text{-}sec^{-1}$

$M_u = \frac{1}{I_2} \frac{\partial M_2}{\partial u}$, $m^{-1}\text{-}sec^{-1}$

$M_\alpha = \frac{1}{I_2} \frac{\partial M_2}{\partial \alpha}$, $rad^{-1}\text{-}sec^{-2}$

$M_{\dot{\alpha}} = \frac{1}{I_2} \frac{\partial M_2}{\partial \dot{\alpha}}$, $rad^{-1}\text{-}sec^{-1}$

$M_{\delta_e} = \frac{1}{I_2} \frac{\partial M_2}{\partial \delta_e}$, $rad^{-1}\text{-}sec^{-2}$

M_1, M_2, M_3 moments about x_1, x_2, and x_3, N-m

m mass, kg

P period, sec

p,q,r angular velocities about x_1, x_2, and x_3, $rad\text{-}sec^{-1}$

S wing area, m^2

s Laplace operator

$T_{1/2}$ time to damp to half amplitude, sec

T_{double} time to double amplitude, sec

t time, sec

U_0 steady-state part of $\vec{V}_A$ in stability axes, $m\text{-}sec^{-1}$

u changing part of $\vec{V}_A$ in stability axes, $m\text{-}sec^{-1}$

V airplane speed along stability axes, $m\text{-}sec^{-1}$

$\vec{V}_A$ airplane velocity vector, $m\text{-}sec^{-1}$

$\vec{V}_E$ vector acceleration in Earth-fixed axes, $m\text{-}sec^{-2}$

$\vec{V}_R$ resultant velocity vector, $m\text{-}sec^{-1}$

$\vec{V}_w$ wind velocity vector, $m\text{-}sec^{-1}$

$V_{G,1}, V_{G,2}, V_{G,3}$ components of $\vec{V}_A$ in Earth-fixed axes, $m\text{-}sec^{-1}$

v_1, v_2, v_3 components of $\vec{V}_A$ along x_1, x_2, and x_3, $m\text{-}sec^{-1}$

$v_{w,1}, v_{w,2}, v_{w,3}$ components of $\vec{V}_w$ along X_1, X_2, and X_3, m-sec^{-1}

$v'_{w,1}, v'_{w,2}$ wind gradients with altitude, sec^{-1}

$v'_{w,3}$ wind gradient along flight path, sec^{-1}

W_i initial wind speed, m-sec^{-1}

X_u $= \frac{1}{m} \frac{F_{y,1}}{\partial u}$, sec^{-1}

X_α $= \frac{1}{m} \frac{F_{y,1}}{\partial \alpha}$, m-rad^{-1}-sec^{-2}

X_{δ_e} $= \frac{1}{m} \frac{F_{y,1}}{\partial \delta_e}$, m-rad^{-1}-sec^{-2}

X_1, X_2, X_3 Earth-fixed axes

X'_1, X'_2, X'_3 nonrotating axes that translate with air and are always parallel to X_1, X_2, and X_3

x_1, x_2, x_3 airplane principal body axes

y_1, y_2, y_3 stability axes

Z_q $= \frac{1}{m} \frac{F_{y,3}}{\partial \theta}$, m-rad^{-1}-sec^{-1}

Z_u $= \frac{1}{m} \frac{F_{y,3}}{\partial u}$, sec^{-1}

Z_α $= \frac{1}{m} \frac{F_{y,3}}{\partial \alpha}$, m-rad^{-1}-sec^{-2}

$Z_{\dot{\alpha}}$ $= \frac{1}{m} \frac{F_{y,3}}{\partial \dot{\alpha}}$, m-rad^{-1}-sec^{-1}

Z_{δ_e} $= \frac{1}{m} \frac{F_{y,3}}{\partial \delta_e}$, m-rad^{-1}-sec^{-2}

α angle of attack, $\alpha_0 + \Delta\alpha$, rad

α_0 steady-state angle of attack, rad

$\Delta\alpha$ change in angle of attack, rad

β angle of sideslip, rad

Γ flight-path angle, $\Gamma_0 + \gamma$, rad

Γ_c flight-path command - rad

Γ_0 steady-state flight-path angle, rad

γ change in flight-path angle, rad

δ_e elevator deflection, rad

δ_f flap deflection, rad

ζ_p phugoid damping ratio

θ Euler pitch angle, rad

ρ air density, $kg\text{-}m^{-3}$

σ_T total shear parameter

σ_u vertical wind shear parameter

σ_w downdraft-updraft parameter

τ servo time constant in flight-path control system - sec

τ_E servo time constant in speed control system - sec

φ Euler roll angle, rad

ψ Euler yaw angle, rad

$\vec{\omega}$ airplane angular velocity vector, $rad\text{-}sec^{-1}$

ω_p phugoid natural frequency, rad - sec^{-1}

Subscript:

i initial

Dots over symbols indicate differentiation with respect to time. An arrow over a symbol denotes a vector.

ANALYSIS

Work in wind shear is somewhat complicated by the lack of positive definitions; therefore, it is necessary to define exactly what is meant by the terminology used herein. Vertical wind shear is the change of the horizontal components of the wind with altitude and is referred to as wind shear. Head winds are negative and tail winds are positive. A positive wind shear gives a decreasing head wind or changes a head wind into a tail wind. A negative wind shear gives a decreasing tail wind or changes a tail wind into a head wind. This definition is maintained whether the airplane is climbing or diving.

The variation of wind speed with altitude that occurred on the approach path at John F. Kennedy International Airport at New York on June 24, 1975, is shown in figure 1. The data given in figure 1 were recorded about the time of the crash of Eastern Airlines Flight Number 66 and, because the wind gradient $v'_{W,1}$ exceeds 0.1 sec^{-1}, these data represent a severe wind shear. In figure 1, head winds are negative and tail winds are positive. From 178 m to 116 m there are rapidly changing head winds. At an altitude of 116 m, a well-defined shear starts and continues down to 50 m. Table I shows the $v'_{W,1}$ that existed over various altitude intervals. (See fig. 1.)

TABLE I.- WIND SHEAR GRADIENTS

[Taken from fig. 1]

Altitude interval, m	$v'_{W,1}$, sec^{-1}
116 to 102	0.10
102 to 80	.35
80 to 68	.09
68 to 50	.27
Average over altitude range . . .	0.20

A useful parameter in the analysis of wind shear is the wind shear parameter σ_u. This parameter which comes from the linearization of the equations of motion (see appendix A) is defined as

$$\sigma_u = \frac{U_0 v'_{W,1}}{g} \tag{1}$$

When equation (1) is applied to the gradient given in table I, it is found that for a typical commercial jet with an approach speed of 77.12 m-sec^{-1}, σ_u varies from 0.79 to 2.75.

When a vertical wind shear, that is, the variation of horizontal wind speed with altitude, occurs in a thunderstorm, it is likely to be accompanied by updrafts and downdrafts. Severe downdrafts are sometimes referred to as downblasts. The updrafts and downdrafts that occurred along the approach path at Kennedy Airport at the same time as the vertical shear shown in figure 1 are presented in figure 2. The corresponding parameter for an updraft or downdraft is

$$\sigma_w = \frac{U_0 v'_{W,3}}{g} \tag{2}$$

where $v'_{W,3}$ is the gradient. Figure 2 was used to determine gradients for the downdrafts and updrafts and the gradients were found to vary between 0.05 sec^{-1} to -0.06 sec^{-1}. The corresponding values of σ_w were 0.31 and -0.47. The data obtained from figures 1 and 2 and reference 8 were used in the analysis of the longitudinal stability of a large four-engine jet transport. The characteristics of this airplane and the flight conditions used are given in appendix B.

The changing wind speed imparts an acceleration to the reference system (that is, the nonrotating axes that translate with the airplane); thus, this axis system is no longer inertial and Earth-fixed axes must be used. The total acceleration $\vec{V}_E$ is given by

$$\dot{\vec{V}}_E = \dot{\vec{V}}_A + \dot{\vec{V}}_W \tag{3}$$

A set of longitudinal equations of motion based on equation (3) are given in reference 7. These equations take into account vertical wind shear, but downdrafts and updrafts are not considered. In appendix A, the equations presented in reference 7 are extended to include the effects of downdrafts and updrafts. Equation (A18) was used to study the longitudinal stability of a large jet transport. The total shear parameter σ_T is introduced in equation (A18). This parameter is defined as

$$\sigma_T = \sigma_u + \sigma_w \tag{4}$$

In order to obtain a clear understanding of the effects of vertical wind shear, the analysis was made with $\sigma_w = 0$, and the effects of σ_w were considered after the vertical shear study.

Equation (A18) is very interesting as the presence of σ_T and σ_w in the dynamic terms indicates an interaction between the airplane and its environment. This equation was used to make a stability analysis of the large four-engine jet transport described in appendix B. The analysis was made for flight-path angles for 0 to ±0.1745 rad in steps of 0.01745 rad. The range of values for σ_T ($-3.5 \leq \sigma_T \leq 3.5$) was based on the wind shear data presented in figure 1.

The left-hand side of equation (A18) was used to obtain the characteristic equation of the airplane, a quartic, which was solved to determine the stability. The results obtained for $\Gamma_0 = -0.05236$ rad are given in table II. Figure 3, a root-locus plot based on table II, shows the motion of the roots as σ_T changes. The data presented in table II and figure 3 show that negative wind has little effect on the airplane. In the case of positive shear, these data indicated no appreciable effect on the phugoid until σ_T exceeds 1.0. At $\sigma_T = 1.0$, the phugoid has broken down into two aperiodic modes, one of which is unstable. The stable mode damps to half amplitude in about 54 sec, whereas the unstable mode takes 333 sec to double amplitude. As σ_T increased above 1.0, the time to double amplitude decreased until it was 3.1 sec for $\sigma_T = 3.5$. The results for the other flight-path angles used in the study were consistent with those obtained for $\Gamma_0 = -0.05236$ rad.

The breakdown of the phugoid oscillation into two aperiodic modes for $\sigma_T \approx 1.0$ was traced to the term $g(\cos \Gamma_0 - \sigma_T \cos 2\Gamma_0)$ which changes sign at this value of σ_T. The change in sign of this term is independent of the sign of Γ_0 so the same type of instability will occur whether $\sigma_T \geq 1.0$ for climbing and level flight. A more complete discussion of this term is given in appendix C. The effect of wind shear on the short-period longitudinal modes was negligible. The short-period roots were periodic $-0.70058998 \pm 0.80948427i$ for $\Gamma_0 = \sigma_u = 0$ and $-0.68874419 \pm 0.78130806i$ for $\Gamma_0 = -0.05236$ and $\sigma_u = 3.5$. Increasing the flap deflection to 0.87266 rad produced very little or no change in these results.

TABLE II.- EFFECT OF POSITIVE AND NEGATIVE SHEAR

ON PHUGOID MODE - BASIC AIRPLANE

$[\delta_f = 0.4363$ rad; $\sigma_w = 0.0]$

Γ_0, rad	σ_u	Roots		$T_{1/2}$, sec	T_{double}, sec	P, sec	ω_p, rad	ζ_p
0.0	0.0	-0.002954	±0.14028i	234.59	------	44.79	0.14031	0.021
-.05236	.0	-.0052453	±.14050i	132.09	------	44.72	.1406	.037
↓	-.5	-.0052994	±.17147i	130.77	------	36.64	.1716	.031
	-1.0	-.0054139	±.19725i	128.00	------	31.85	.1973	.027
	-1.5	-.0055879	±.21969i	124.02	------	28.60	.2198	.025
	-2.0	-.0058200	±.23974i	119.07	------	26.21	.2398	.024
	-2.5	-.0061076	±.25797i	113.47	------	24.36	.2580	.024
	-3.0	-.0064496	±.27475i	107.45	------	22.87	.2748	.023
	-3.5	-.0068442	±.29032i	101.25	------	21.64	.2904	.023
	.5	-.0052567	±.099619i	131.83	------	63.07	.9962	.0528
	1.0	-.012747	.0020821		332.84	-----	------	-------
	1.5	-.10647	.095524		7.25	-----	------	-------
	2.0	-.14893	.13756		5.04	-----	------	-------
	2.5	-.18207	.17013		4.07	-----	------	-------
	3.0	-.21051	.19785		3.50	-----	------	-------
	3.5	-.23600	.22249		3.11	-----	------	-------

Phugoid Stability Boundary

As pointed out in the previous section, a study of the calculations that produced table II showed that unstable conditions occur when the term $g(\cos \Gamma_0 - \sigma_T \cos 2\Gamma_0)$ in equation (A18) changes sign. The only possible way in which this term can change sign is for σ_T to become greater than a critical value. For $\Gamma_0 = 0$, the critical value of σ_T is 1.0. Additional calculations showed that for the normal range of flight-path angles, the difference between the critical value of σ_T and 1.0 was negligible. These results lead to a stability boundary for the phugoid in wind shears that is independent of airplane characteristics. (See appendix C.) This boundary is obtained by setting equation (1) equal to 1.0 and solving for $v'_{w,1}$ as a function of the speed. This boundary is shown in figure 4(a). The approach speed bands for general aviation and jet transports have been marked in figure 4(a). A glance at figure 4(a) reveals that the higher the speed of the airplane, the smaller the wind gradient for the onset of unstable conditions. Because of the slower approach speeds, general aviation aircraft can tolerate a higher gradient, before becoming unstable, than transport aircraft. As there were no airplane characteristics used to determine the curve shown in figure 4(a), it is necessary to assume a specific airplane in order to determine stability conditions around the stability boundary.

A segment of the curve from 50 m-sec^{-1} to 100 m-sec^{-1} is shown in figure 4(b). Times to double amplitude (above the curve) and times to half amplitude (below the curve) have been calculated for the airplane described in appendix B at three specific speeds, 67 m-sec^{-1}, 77 m-sec^{-1}, and 87 m-sec^{-1}, as a function of wind gradient. This speed range covers the approach speeds for jet transports. As would be expected, the time to double amplitude decreases as the gradient increases. As the speed is increased for a given value of $v'_{W,1}$ that is near the stability boundary curve, changes in stability are most drastic. For $v'_{W,1} = 0.15$ the time to double the amplitude decreases from 35.1 sec at 67 m-sec^{-1} to 8.9 sec at 87 m-sec^{-1}. At $v'_{W,1} = 0.125$, the phugoid changes from stable to unstable over this speed range. These results are interesting as they indicate that the phugoid stability can be helped by slowing the airplane down, a practice not recommended because the airplane is approaching its stall speed. On the other hand, increases in speed, particularly for gradients close to those for $\sigma_T = 1.0$, can cause an unstable condition to develop.

Use of Automatic Pilots

Automatic pilots offer a means of improving the airplane characteristics when it is flying through wind shear. There are two basic types of autopilot that can be used to control longitudinal motion. These are a θ autopilot that controls pitch attitude and a Γ autopilot that controls the flight path of the airplane. The θ autopilot was not considered for the following reasons:

(1) During landing approach, a constant flight path is desired and a θ autopilot provides only indirect control of the flight path.

(2) A θ autopilot places a constraint on the pitch attitude of the airplane and forces all flight-path variations into the angle of attack. The variations in α can have an adverse effect on lift and may even cause the airplane to stall.

A block diagram of the Γ autopilot used in this study is presented in figure 5.

There are four gains and a servo time constant to be assigned values. The values used are

$$k = 0.8$$

$$k_1 = 5.0$$

$$k_2 = 1.0$$

$$k_3 = 7.7$$

$$\tau = 0.0357$$

and were taken from the successful Γ autopilot used in reference 9. By using these gains and the data presented in appendix B, the roots of the characteristic equations were determined for the same range of Γ_0 and σ_T as the basic

airplane or in table II. The characteristic equation is a six-degree equation. Again, these calculations were made with $\sigma_w = 0.0$. The negative wind shear case will be considered first. A typical set of roots when $\Gamma_0 = -0.05236$ rad and $\sigma_T = -1.00$ are .

0.012992936

-0.27539026 ± 0.14547961i

-0.46845553 ± 2.127338i

-27.956636

The two periodic roots damp to half amplitude in 2.52 and 1.48 sec, respectively. The stable aperiodic root damps to half amplitude in about 0.025 sec and it takes the unstable aperiodic root about 53 sec to double amplitude. This root pattern was constant throughout the negative shear calculations. The unstable condition comes from the term

$$\left[\left(-\frac{\sigma_T g}{2U_0}\sin 2\Gamma_0 - X_u\right)\left(-Z_\alpha\right) - \left(-Z_u - \frac{\sigma_T g}{U_0}\sin^2\Gamma_0\right)(-X_\alpha)\right]M_{\delta_e} kk_2 \tag{5}$$

which is the constant term in the characteristic equation of the airplane autopilot system with X_{δ_e} and Z_{δ_e} set equal to zero. The foregoing results were consistent over the range of negative shear and flight path considered in the study.

When the wind shear was positive, the same root pattern was found for small values of Γ_0 and σ_T. For $\Gamma_0 = -0.05235$ and $\sigma_T = 1.0$, the roots are

0.00099216978

-0.27327956 ± 0.12053726i

-0.45804227 ± 2.1141669i

-27.956737

which, with the exception of the unstable root, are very close to the roots obtained for negative shear. When the shear factor was increased to 1.5, the airplane autopilot combination became stable and the roots are

-0.0024078146

-0.27256525 ± 0.11293999i

-0.455542571 ± 2.1108572i

-27.956762

This small change in stability occurred because the term $(\sigma_T g/2U_0)\sin 2\Gamma_0$ has become large enough to change when combined with $-X_u$, the sign of the con-

stant term (expression (5)); thus, a stable system is obtained. The foregoing calculations were made with X_{δ_e} and Z_{δ_e} equal to zero. Both cases were rerun with estimated values for these parameters and no significant changes were found in the results. The results obtained for positive shear were most interesting as a wind shear that destabilized the phugoid for the airplane alone now exerted a stabilizing effect for the airplane autopilot combination.

Because the unstable mode in the airplane-autopilot system occurred for $\Gamma_0 = \sigma_T = 0.0$, this condition indicated that the source of the problem was the airplane-autopilot system and not the wind shear.

For $X_{\delta_e} = Z_{\delta_e} = 0$ and $\sigma_T = \Gamma_0 = 0$, the constant term in the characteristic equation of the airplane autopilot system is $(X_u Z_\alpha - Z_u X_\alpha) M_{\delta_e} k k_2$ and the unstable condition occurs for the configuration used in this study, because $Z_u X_\alpha$ is greater than $X_u Z_\alpha$. An increase in $X_u Z_\alpha$ will restore stability. For the airplane used, this increase in $X_u Z_\alpha$ can be obtained by increasing the flap deflection from 0.4363 rad to 0.87266 rad. This doubling of the flap deflection gives $X_u Z_\alpha = 2.40642$ and $Z_u X_\alpha = 1.88339$ and results in a positive difference and a completely stable airplane autopilot combination. The roots of the characteristic equation for $\Gamma_0 = 0.05235$ rad and a negative shear factor $\sigma_T = -1.0$ are

$$-0.0028802057$$

$$-0.27307666 \pm 0.15105564i$$

$$-0.48581279 \pm 2.1097746i$$

$$-27.949297$$

The instability just discussed arises because of the flight-path constraint imposed on the airplane by the flight-path control system. This type of instability, stability under partial constraint, is discussed in detail in references 10 and 11. The method used to eliminate it, that is, increasing flap deflection, is the same as that suggested in reference 12.

When the shear factor increased to -1.5, an unstable root again appeared in the characteristic equation. The shortest time to double amplitude was approximately 124 sec, a length of time that should pose no problems of control. Depending on the value of Γ_0, the transition from stable to unstable conditions occurs at different values of σ_T; the smaller Γ_0, the larger the σ_T required to cause an instability. When the shear factor was positive, $\sigma_T = 1.0$; for the same Γ_0 the roots of the characteristic equation are

$$-0.016587880$$

$$-0.26976410 \pm 0.12312273i$$

$$-0.47574423 \pm 2.0964192i$$

$$-27.949405$$

Over the range of Γ_0 and σ_T considered in the investigation, the airplane autopilot system remained stable; however, as both Γ_0 and σ_T increased, the size of the first real root increased and decreased the time to damp to half amplitude.

Updrafts and Downdrafts

As pointed out at the beginning of the analysis section, updrafts and downdrafts can occur (see fig. 2) in conjunction with vertical wind shear. Like vertical wind shear, gradients can occur in upward and downward vertical velocities. An analysis of the measured data presented in figure 2 showed gradients from 0.06 sec^{-1} to 0.05 sec^{-1}. For these gradients, the downdraft parameter lies in the range $-0.47 \leq \sigma_w \leq 0.31$.

When σ_w is included in the equations of motion, it appears as an additive factor to σ_u, $\sigma_T = \sigma_u + \sigma_w$, except in the coefficient of the u term of the second equation of equation (A18). In this coefficient the term $(g/U_0)\sigma_w$ appears with no corresponding σ_u term. The effect of this term on the results is negligible. For instance, let $\sigma_u = 2.0$ and $\sigma_w = 0.4$. Calculations showed that with the $(g/U_0)\sigma_w$ omitted, $\sigma_T = 2.4$ and the predicted time to double amplitude was 4.26 sec. When $(g/U_0)\sigma_w$ was included, the predicted time to double amplitude was 3.82 sec, a change of 0.44 sec which is negligible. Calculations using the range of σ_u and σ_w noted in this report should show similar results. It appears that unless σ_w becomes very large, an excellent approximation of the stability can be obtained if the term $(g/U_0)\sigma_w$ is not considered.

The only change, outside of the summation of σ_u and σ_w, in the quadratic approximation for the phugoid mode is in the expression for ω_p^2 which becomes

$$\omega_p^2 = \frac{g}{U_0}\left\{\left[X_u(\sin\Gamma_0 - \sigma_T \sin 2\Gamma_0) - \left(Z_u - \frac{g}{U_0}\sigma_w\right)(\cos\Gamma_0 - \sigma_T \cos 2\Gamma_0)\right]\right\} \qquad (6)$$

where $\sigma_T = \sigma_u + \sigma_w$. If $(g/U_0)\sigma_w > Z_u$ the stability is still determined by the sign of $\cos\Gamma_0 - \sigma_T \cos 2\Gamma_0$. If, however, $(g/U_0)\sigma_w < Z_u$, sign changes will occur that will affect the prediction of stability. Since $(g/U_0)\sigma_w = v'_{w,3}$, this means that $v'_{w,3}$ would have to be less than -0.3. For the severe wind condition used in this report $v'_{w,3}$ did not exceed ± 0.1 sec^{-1}. As Z_u varies from -0.15 to -0.40 for most airplanes, it is concluded that only in rare instances will the term $(g/U_0)\sigma_w$ influence the stability calculated from equation (A18) and the phugoid approximation.

The phugoid stability boundary (fig. 4(a)) is based on the zeros of ω_p^2 in that ω_p^2 will change sign for $\sigma_T > 1.0$. This boundary was recalculated by using equation (6) and it was found that over the range of σ_w values considered in this paper (which are for severe weather conditions), $(g/U_0)\sigma_w$ did not change the result that over a normal range of flight-path angles, the sign of ω_p^2 is dependent on σ_T. Thus, for most σ_w the phugoid stability boundary of figure 4(a) is valid.

DISCUSSION

In the preceding section, an analysis of the longitudinal stability of a large transport airplane in wind shear was made. The results of this analysis definitely show an interaction of the airplane and its environment. The interaction comes from accelerations produced by the wind gradient. The gradient is the important wind factor, not the wind speed. These facts made the results obtained difficult to interpret because the classical stability conditions are concerned with the stability about a steady-state condition and wind shear is a transient phenomenon. The equations used for the analysis give the stability over regions of constant wind shear.

The results of the stability analysis show that shear, particularly positive shear, can have a drastic effect on the stability of an airplane. In order for the pilot to take action, it is necessary for him to know whether a wind shear is present and what type (that is, positive or negative) wind shear is affecting the airplane. References 13 and 14 attack the problem of measuring the total energy rate of the airplane and describe devices for its measurement, the one described in reference 13 being particularly simple and effective and suitable for general aviation aircraft. Reference 14 goes one step beyond reference 13 and shows how the change in total energy can be used to detect wind shears.

Control-Fixed Aircraft Motions in Wind Shear

In order to obtain better insight into the meaning of the results obtained from the analysis made with the stability equations, the six-degree-of-freedom equations (see appendix A) were reduced to the three-degree-of-freedom equations of longitudinal motion with $\sigma_w = 0.0$ and programed for digital computations of aircraft motions.

In all cases, including those with head winds and tail winds, the airplane was trained on a -0.05236 rad flight path at an altitude of 130 m. Thus, the only disturbances that occur during the flight are the vertical wind shears that start at an altitude of 106 m and end at an altitude of 50 m.

Plots of altitude, pitch angle, and flight path against D are shown in figure 6. The distance along the approach path D was used instead of time for the plotting since this distance relates the motions to the space position of the airplane. All the motions shown in figure 6 are for fixed controls. Curve A, which is for zero initial wind speed, $W_i = 0$, and $\sigma_T = 0.0$, is taken as the reference case. A 6.1-m-sec^{-1} head wind (curve B) causes the airplane to undershoot and the glide slope becomes a little steeper; the pitch angle is larger, but remains relatively constant.

When a tail wind of 6.1 m-sec^{-1} is encountered (curve C), the airplane floats and the flight path is not as steep as the reference case. As would be expected, the magnitude of the pitch angle is less than was found for the reference condition of curve A. In all three cases the curves are smooth and do not exhibit oscillatory characteristics. The remaining cases (curves D to G) show the effects of shear when combined with a head wind or tail wind. Curves D and

E are for head winds and curves F and G are for tail winds. In all cases the shear started at an altitude of 106 m and continued until the airplane reached an altitude of 50 m where the airplane flew out of the shear. In the case of strong positive shear, $\sigma_T \approx 2.0$, the altitude, θ, and γ motions are characteristic of a system with aperiodic roots, one of which is unstable, and the airplane impacts about 1500 m short of the undisturbed impact point. From the onset of the shear, only 7 sec elapsed before impact. When the shear was decreased, $\sigma_T = 0.5$, the characteristic of the traces changed, and the airplane was just starting to level off in what appears to be the start of an oscillating response when impact occurred about 800 m short of the undisturbed touchdown point. The stability analysis for this case predicted an oscillating response and the impact condition is consistent with long time to damp to half amplitude, about 65 sec, predicted by the stability analysis. For curves F and G, W_i was changed to 6.10 $m\text{-}sec^{-1}$ and the shear parameters σ_T were -0.5 and -2.0. As would be expected, the airplane floated and a large overshoot occurred. As predicted by the stability, the response is oscillating but damped, the oscillations being induced by the wind shear which excited the phugoid mode. As a result of these motion studies, the results that were predictable from the stability analysis, that positive shears are most dangerous to aircraft and that negative shears are much less so, have been confirmed.

Many airplanes in the past have been statically unstable in the power approach condition. When such an airplane is allowed to diverge downward with fixed controls, the airspeed increases and the angle of attack decreases. In the case of a down divergence in positive wind shear, however, the airspeed decreases and the angle of attack increases, and the normal recovery technique of the use of up elevator to recover results in stall and further loss of altitude. The divergence due to wind shear, although it affects the constant term of the stability equation the same as static instability, would result in entirely different piloting problems.

Motion results were also obtained for a flap setting at 0.87266 rad instead of 0.43633 rad with little change in the responses of the airplane. The effects of downdrafts and updrafts were found to affect the airplane in the same manner as positive and negative shears, respectively; thus, the shear parameter need only be adjusted to account for this effect.

The usual method for simulating wind, turbulence, and other wind effects, such as shear, in airplane simulations is to include the effects in the resultant velocity vector used in calculating the airplane forces and moments. Terms such as the $\dot{\vec{V}}_W$ terms in equations (A4) to (A6) are generally not included in the equations of motion. These $\dot{\vec{V}}_W$ terms that appear in equations (A4) to (A6) or their equivalent were included in all calculations made in this study. Figures 7 and 8 show the effect of neglecting these terms for positive and negative shear. Although the general character of the motions is the same, the $\dot{\vec{V}}_W$ terms have a significant effect on the airplane motions.

Use of Autopilots To Control Airplane in Wind Shear

The results of the stability analysis indicated that an automatic flight-path control system provided an increase in the stability of the airplane. The

motion study showed that changes in airspeed as large as 23 $m\text{-}sec^{-1}$ were occurring for the shear passage, which implies that an airspeed control is necessary so that the lift of the airplane is maintained as constant as possible. The flight-path and speed-control systems were checked separately before being combined. The flight-path control system (fig. 5) was added to the simulation and the results showed large changes in angle of attack that caused the airplane to stall. Changing the $\dot{\Gamma}$ feedback to a q feedback provided increased stability and eliminated the large excursions in angle of attack. All results presented in the section are for the flight-path control system with a q pitch rate feedback. The speed-control system was set up to keep the resultant speed, that is, the sum of wind-speed vector and ground-speed vector constant. The resultant speed (or airspeed) is available from the air data computer. As shown in figure 9, the engine was simulated by a first-order servo. The time constant of this servo was selected so that 90 percent of the command thrust was achieved in 5.6 sec and a τ_E of 2.5 resulted. This time delay matches well with the engine response data given in figure 28 of reference 15 for engine response to throttle. A τ_E of 0.1 was also used to simulate the thrust modulators of reference 15. The values of τ_E given were assumed to simulate the extremes of engine response. The results of these calculations are shown in figures 10 and 11. The flight-path and airspeed control systems successfully guided the airplane through a wind shear where $\sigma_T = \pm 2.0$. The positive shear case shows more sensitivity to the engine time constant than the negative shear case. The speed control system, through its input command, attempts to hold airspeed constant. In combination with the acceleration feedback, this control system also attempts to hold acceleration to zero. This procedure is roughly the equivalent of attempting to hold $|\vec{V}_R \cdot \vec{V}_R|/g$ constant, which is part of the energy rate equation given in reference 11. Good results were obtained by use of this autopilot. It appears that a critical term to control is $|\vec{V}_R \cdot \vec{V}_R|/g$ and that more work should be done on automatic control systems that directly control this term.

CONCLUDING REMARKS

The effect of the phenomenon of wind shear, that is, the variation of horizontal winds with altitude, on the stability and motions of a large jet transport has been investigated. In the case of the phugoid mode negative wind shear, a shear that changes tail winds to head winds, the phugoid remained periodic and stable, although the time to damp to half amplitude decreased as the shear gradient increased. Positive wind shear, a shear that changes a head wind into a tail wind, caused the phugoid to become unstable for values of the shear parameter greater than 1.0. The motion was aperiodic and the time to double amplitude decreased as the shear parameter increases. In the case of positive wind shear, a stability boundary for the phugoid, valid for all aircraft, was found as a function of the wind gradient and approach speed. The stability boundary is independent of airplane characteristics and, apparently, an attempt to hold airspeed constant in wind shear conditions is the best action to avoid changes in airplane stability.

The effect of wind on airplane motions confirmed the effects predictable from the stability analysis. More study is needed of autopilots for the adequate control during a wind shear encounter. The results indicate that it is

important for the pilot to know whether a wind shear exists and whether it is positive or negative.

Downdrafts and updrafts were considered as well as horizontal wind shears. It was found that downdrafts and updrafts have the same effect as wind shear and could be accounted for by modification of the shear parameter.

A stability analysis of the airplane equipped with a flight-path control autopilot showed that the combination was a stable system. When the shear was negative, increasing the flap deflection helped system stability. Motions obtained with a flight-path control with a pitch-rate feedback and a speed-control system that held constant speed with respect to the air mass showed that with these control systems, an airplane could fly through vertical wind shears with no adverse effects.

Langley Research Center
National Aeronautics and Space Administration
Hampton, VA 23665
April 27, 1977

APPENDIX A

AIRPLANE EQUATIONS OF MOTION USED IN THIS STUDY

The linear accelerations of an airplane in a moving axis system are given by the vector equation

$$\dot{\vec{V}}_E = \frac{d}{dt}(\vec{V}_A + \vec{V}_w) + \vec{\omega} \times (\vec{V}_A + \vec{V}_w)$$

and the corresponding force equations are

$$\frac{d}{dt}(\vec{V}_A + \vec{V}_w) + \vec{\omega} \times (\vec{V}_A + \vec{V}_w) = \frac{\vec{F}}{m} \tag{A1}$$

Equation (A1) is general and may be resolved into any desired coordinate system. Because the use of principal body axes simplifies the resulting equation, these axes were used for the six-degree-of-freedom equations. The wind vector $\vec{V}_w$ is defined in Earth-fixed axes, X_1, X_2, and X_3, head winds are negative, and $\vec{V}_A$ is defined in principal body axes, x_1, x_2, and x_3. The X_1 and x_1 axes are positive in the direction of flight and the X_3 and x_3 axes are positive downward. (See fig. 12.)

In order to obtain the force equations in the principal body axes, it is necessary to transform the wind from the fixed-axis system to the body-axis system. This is done by using the nine direction cosines obtained from the standard ψ, θ, and φ Euler transformation. The direction cosines ℓ_{ij} are obtained from

$$\ell_{ij} = (\ell_{ij})_i + \int_0^t \dot{\ell}_{ij}\, dt \tag{A2}$$

where $\dot{\ell}_{ij}$, the direction cosine rates, are given by

$$\left.\begin{aligned} \dot{\ell}_{i1} &= r\ell_{i2} - q\ell_{i3} \\ \dot{\ell}_{i2} &= p\ell_{i3} - r\ell_{i1} \\ \dot{\ell}_{i3} &= q\ell_{i1} - p\ell_{i2} \end{aligned}\right\} \tag{A3}$$

By using equations (A2) and (A3), equation (A1) may be written in component form as

$$\dot{v}_1 + \dot{v}_{w,1}\ell_{11} + \dot{v}_{w,2}\ell_{21} + \dot{v}_{w,1}\ell_{31} + qv_3 - rv_2 = \ell_{31}g + \frac{F_1}{m} \tag{A4}$$

$$\dot{v}_2 + \dot{v}_{w,1}\ell_{12} + \dot{v}_{w,2}\ell_{22} + \dot{v}_{w,3}\ell_{32} + rv_1 - pv_3 = \ell_{32}g + \frac{F_2}{m} \tag{A5}$$

$$\dot{v}_3 + \dot{v}_{w,1}\ell_{13} + \dot{v}_{w,2}\ell_{23} + \dot{v}_{w,3}\ell_{33} + pv_2 - qv_1 = \ell_{33}g + \frac{F_3}{m} \tag{A6}$$

The variables p, q, and r are the angular velocities of the airplane in principal body axes and are obtained from the equations of angular motion which, in component form, are

$$\dot{p} + \frac{I_3 - I_2}{I_1} qr = \frac{M_1}{I_1} \tag{A7}$$

$$\dot{q} + \frac{I_1 - I_3}{I_2} pr = \frac{M_2}{I_2} \tag{A8}$$

$$\dot{r} + \frac{I_2 - I_1}{I_3} pq = \frac{M_3}{I_3} \tag{A9}$$

The aerodynamic forces and moments are functions of the resultant velocity $\vec{V}_A$ given by

$$\vec{V}_R = \vec{V}_A - \vec{V}_w$$

as are the parameters α, $\dot{\alpha}$, β, and $\dot{\beta}$. Because of the wind shear stability derivatives normally neglected (such as C_{D_u}, C_{m_u}, C_{n_u}, C_{Z_φ}, and C_{n_φ}) should be included in the formulation of the forces and moments. The wind vector $\vec{V}_w$ includes steady winds, turbulence, and wind shear. Head winds are negative.

An examination of equations (A4) to (A6) indicated that in addition to the usual terms, the terms $\dot{v}_{w,1}$, $\dot{v}_{w,2}$, and $\dot{v}_{w,3}$ are required. These terms are wind acceleration terms and may arise from turbulence or wind shear. In models for turbulence, it is fairly easy to write the model so that the accelerations are available for equations (A4) to (A6). In the case of wind shears, particularly where recordings of actual wind shears are used, obtaining the required accelerations is not quite so straightforward. In order to have a consistent method of specifying wind shears, the following method is suggested. An acceleration may be written as a product of a velocity gradient taken over some characteristic length and the rate of change of this length. Thus,

$$a = \frac{dv}{d\ell} \frac{d\ell}{dt} \tag{A10}$$

The length ℓ over which the gradient is determined should be 30.48 m, a length that is consistent with the reporting of vertical wind shears. Thus, winds separated by 30.48 are subtracted and divided by 30.48 to obtain $dv/d\ell$ which has the dimensions of sec^{-1}. Thus, wind accelerations for equations (A4), (A5), and (A6) are given by

$$\dot{v}_{w,1} = \frac{dv_{w,1}}{d\ell} V_{G,3} \tag{A11}$$

$$\dot{v}_{w,2} = \frac{dv_{w,2}}{d\ell} V_{G,3} \tag{A12}$$

$$\dot{v}_{w,3} = \frac{dv_{w,3}}{d\ell} V_{G,1} \tag{A13}$$

where $dv_{w,1}/d\ell$, $dv_{w,2}/d\ell$, and $dv_{w,3}/d\ell$ are the velocity gradients and usually written as $v'_{w,1}$, $v'_{w,2}$, and $v'_{w,3}$.

Equations (A4), (A6), and (A8) are the longitudinal equations of motion and were used to calculate the airplane motions presented in this report.

For the stability calculations presented in this paper, the longitudinal equations of motion were transformed to stability axes. (See fig. 12.) After making this transformation and substituting the trigonometric equivalents for the direction cosines and using the definition of Γ, $\Gamma = \theta - \alpha$, the longitudinal equations of motion in stability axes are

$$\dot{V} - v'_{w,1} \sin \Gamma \cos \Gamma - v'_{w,3} \cos \Gamma + g \sin \Gamma = \frac{F_{y,1}}{m} \tag{A14}$$

$$-V\dot{\Gamma} - v'_{w,1} V \sin^2 \Gamma + v'_{w,3} V \cos^2 \Gamma - g \cos \Gamma = \frac{F_{y,3}}{m} \tag{A15}$$

$$\ddot{\Gamma} + \ddot{\alpha} = \frac{M_2}{I_2} \tag{A16}$$

In these equations $\vec{V}_A$ is now a single component vector in the y_1-direction in stability axes, and called V. Equations (A14) to (A16) were linearized by making the usual assumptions that

$$V = U_0 + u$$

$$\alpha = \alpha_0 + \Delta\alpha$$

$$\Gamma = \Gamma_0 + \gamma$$

where the zero subscripted terms are the steady state and u, $\Delta\alpha$, and γ are the perturbations from the steady state. For the linearized equations, it is convenient to use σ_u and σ_w which are constants in place of $v'_{w,1}$ and $v'_{w,3}$. These parameters are defined as

$$\sigma_u = \frac{U_0 v'_{w,1}}{g}$$

$$\sigma_w = \frac{U_0 v'_{w,3}}{g}$$

APPENDIX A

The linearized equations of motion are

$$\left.\begin{aligned}
&\left[\frac{d}{dt} - \left(\frac{g\sigma_u}{2U_0} + \frac{g\sigma_w}{2U_0}\right)\sin 2\Gamma_0\right]u + \left\{g\left[\cos\Gamma_0 - (\sigma_u + \sigma_w)\cos 2\Gamma_0\right]\right\}\gamma = \frac{F_{y,1}}{m} \\
&\left(-\frac{g\sigma_u}{U_0}\sin^2\Gamma_0 + \frac{g\sigma_w}{U_0}\cos^2\Gamma_0\right)u + \left\{-U_0\frac{d}{dt} + g\left[\sin\Gamma_0\right.\right. \\
&\left.\left. - (\sigma_u + \sigma_w)\sin 2\Gamma_0\right]\right\}\gamma = \frac{F_{y,3}}{m} \\
&\frac{d^2}{dt^2}(\gamma + \Delta\alpha) = \frac{M_2}{I_2}
\end{aligned}\right\} \quad (A17)$$

The forces and moments were expanded and in matrix form these equations, writing α for $\Delta\alpha$ and σ_T for $\sigma_u + \sigma_w$, become

$$\begin{bmatrix}
\frac{d}{dt} - \frac{g}{2U_0}\sigma_T \sin 2\Gamma_0 - X_u & -X_\alpha & g(\cos\Gamma_0 - \sigma_T\cos 2\Gamma_0) \\
-Z_u - \frac{g}{U_0}(\sigma_T\sin^2\Gamma_0 - \sigma_w) & -(Z_{\dot\alpha} + Z_q)\frac{d}{dt} - Z_\alpha & -(U_0 + Z_q)\frac{d}{dt} + g(\sin\Gamma_0 - \sigma_T\sin 2\Gamma_0) \\
-M_u & \frac{d^2}{dt^2} - (M_{\dot\alpha} + M_q)\frac{d}{dt} - M_\alpha & \frac{d^2}{dt^2} - M_q\frac{d}{dt}
\end{bmatrix}
\begin{bmatrix} u \\ \alpha \\ \gamma \end{bmatrix} =
\begin{bmatrix} X_{\delta_e} \\ Z_{\delta_e} \\ M_{\delta_e} \end{bmatrix}\delta_e \quad (A18)$$

For $\sigma_w = 0$, these equations reduce to the equations given in reference 8 and for $\sigma_T = \sigma_w = 0$, they become the usual longitudinal equations of motion.

APPENDIX B

AIRPLANE CHARACTERISTICS AND FLIGHT CONDITION

The airplane used in this study is considered a typical narrow body modern jet transport airplane powered by four engines, each having approximately 67 233 N of thrust.

The dimensional and mass characteristics are

$\bar{c}$ = 7.01 m

S = 267.9 m^2

m = 90 909.1 kg

I_2 = 9 933 300 kg-m^2

ρ = 1.2929 kg-m^{-3}

The aerodynamic data for the stability axes, center of gravity at 0.25$\bar{c}$, are

	0.43633 rad flap	0.87266 rad flap
Z_α	-55.055 m-rad^{-1}-sec^{-2}	-52.68 m-rad^{-1}-sec^{-2}
Z_u	-0.29024 sec^{-1}	-0.29024 sec^{-1}
Z_q	-3.2708 m-rad^{-1}-sec^{-1}	-3.2708 m-rad^{-1}-sec^{-2}
$Z_{\dot{\alpha}}$	-1.0075 m-rad^{-1}-sec^{-1}	-1.0075 m-rad^{-1}-sec^{-1}
Z_{δ_e}	-2.63428 m-rad^{-1}-sec^{-2}	-2.63428 m-rad^{-1}-sec^{-2}
X_α	-5.9803 m-rad^{-1}-sec^{-2}	-6.48907 m-rad^{-1}-sec^{-2}
X_u	-0.02385 sec^{-1}	-0.04568 sec^{-1}
X_{δ_e}	-0.1568 m-rad^{-1}-sec^{-2}	-0.1568 m-rad^{-1}-sec^{-2}
M_α	-0.809 rad^{-1}-sec^{-2}	-0.8468 rad^{-1}-sec^{-2}
M_q	-0.513 rad^{-1}-sec^{-1}	-0.5481 rad^{-1}-sec^{-1}
$M_{\dot{\alpha}}$	-0.175 rad^{-1}-sec^{-1}	-0.18778 rad^{-1}-sec^{-1}
M_u	-0.00095 m^{-1}-sec^{-1}	-0.00095 m^{-1}-sec^{-1}
M_{δ_e}	-0.73733 rad^{-1}-sec^{-2}	-0.75038 rad^{-1}-sec^{-2}

APPENDIX B

The basic flight condition used was a landing approach along a 3^{o} glide slope with flaps set at 0.43633 rad. The approach speed was 77.12 $m\text{-}sec^{-1}$, the speed recommended by the manufacturer.

APPENDIX C

PHUGOID STABILITY IN WIND SHEAR

The phugoid mode may be approximated by assuming that contributions of the inertial terms and aerodynamic damping terms to the total applied moment are much smaller than those due to changes in u and α. Under these assumptions and for $\sigma_w = 0$, the stability determinant obtained from equation (A18) reduces to

$$\begin{bmatrix} s - \frac{1}{2}\frac{g\sigma_u}{U_0}\sin 2\Gamma_0 - X_u & -X_\alpha & g(\cos\Gamma_0 - \sigma_u \cos 2\Gamma_0) \\ -Z_u - \frac{g\sigma_u}{U_0}\sin^2\Gamma_0 & -Z_\alpha & -U_0 s + g(\sin\Gamma_0 - \sigma_u \sin 2\Gamma_0) \\ -M_u & -M_\alpha & 0 \end{bmatrix} = 0 \qquad (C1)$$

This determinant expands to an equation of the form

$$s^2 + 2\zeta_p\omega_p s + \omega_p^2 = 0 \qquad (C2)$$

where

$$2\zeta_p\omega_p = -X_u + M_u\frac{X_\alpha}{M_\alpha} - \frac{g\sin\Gamma_0}{U_0}(1 - \sigma_u\cos\Gamma_0) \qquad (C3)$$

and

$$\omega_p^2 = \frac{g}{U_0}\left[\left(X_u - M_u\frac{X_\alpha}{M_\alpha}\right)(\sin\Gamma_0 - \sigma_u\sin 2\Gamma_0) - \left(Z_u - M_u\frac{Z_\alpha}{M_\alpha}\right)(\cos\Gamma_0 - \sigma_u\cos 2\Gamma_0)\right] \qquad (C4)$$

As M_u for most aircraft is extremely small or zero, the expressions for $2\zeta_p\omega_p$ and ω_p^2 may be further simplified by neglecting the terms that contain M_u. When the M_u terms are omitted, the expressions for $2\zeta_p\omega_p$ and ω_p^2 become

$$2\zeta_p\omega_p = -X_u - \frac{g}{U_0}\sin\Gamma_0(1 - \sigma_u\cos\Gamma_0) \qquad (C5)$$

$$\omega_p^2 = \frac{g}{U_0}\left[X_u(\sin\Gamma_0 - \sigma_u\sin 2\Gamma_0) - Z_u(\cos\Gamma_0 - \sigma_u\cos 2\Gamma_0)\right] \qquad (C6)$$

APPENDIX C

Since the characteristic equation (C2) is a quadratic, both $2\zeta_p\omega_p$ and ω_p^2 must be positive to guarantee the asymptotic stability of the phugoid; otherwise, at least one root of the equation will have a nonnegative real part so that the phugoid will be unstable. The curves for $2\zeta_p\omega_p = 0$ and $\omega_p^2 = 0$ as functions of Γ_0 and σ_u are shown in figures 13 and 14. These curves were calculated by using equations (C5) and (C6) with appropriate data from appendix B. This information is combined to determine the regions where equation (C2) would be stable or unstable. The regions of stability and instability are shown in figure 15 as functions Γ_0 and σ_u. Most flight-path angles lie in the interval $-(\pi/18) \leqq \Gamma_0 \leqq \pi/18$, which is the region between the vertical lines in figure 15. This figure clearly shows the effect of wind shear σ_u on the phugoid stability in landing ($\Gamma_0 < 0$) and level flights ($\Gamma_0 = 0$). In this case, the airplane is stable for all wind shears that have $\sigma_u < 1.0$. However, for climbing flights ($\Gamma_0 > 0$), the region of stability is much more restricted for negative wind shears.

That the unstable condition for $\sigma_u > 0$ in figure 15 is solely a function of σ_u and not a function of the airplane parameters can be seen by rewriting equation (C6) as

$$\omega_p^2 = \frac{gX_u}{U_0}\left[(\sin\Gamma_0 - \sigma_u \sin 2\Gamma_0) - (\cos\Gamma_0 - \sigma_u \cos 2\Gamma_0)\frac{Z_u}{X_u}\right] \tag{C7}$$

Since Z_u/X_u is the lift-drag ratio of the airplane and is positive with normal values between 5 and 16, it can be shown that the sign of ω_p^2 depends on the sign of $\cos\Gamma_0 - \sigma_u \cos^2\Gamma_0$. To a good degree of accuracy, this means for normal flight-path angles that a value of $\sigma_u > 1.0$ will cause the airplane to have an unstable phugoid mode. This result is immediate for a small angle approximation on Γ_0. Thus, it is only necessary to determine those combinations of $v'_{w,1}$ and U_0 that give $\sigma_u = 1.0$ to determine whether the airplane is stable or unstable for positive shear. A curve for estimating this stability is shown in figure 4(a). This is a serious type of instability as it arises from an interaction of the airplane and its environment and no aerodynamic changes to the airplane will correct it.

The instability for negative shear ($\sigma_u < 0$) (see fig. 15) is not a simple function of σ_u as in the case of positive shear. The effect of negative shear on stability can be computed by using equation (C5); however, it is a function of the airplane parameters as X_u appears in equation (C5). Generally speaking, the instability for $\sigma_u < 0$ is a divergent oscillation instead of aperiodic type motion encountered for positive shear ($\sigma_u > 0$).

REFERENCES

1. Brown, David A.: Wind Shear Threat Spurs Drive To Find Remedies. Aviation Week & Space Technol., vol. 104, no. 14, Apr. 5, 1976, p. 32.

2. Aircraft Accident Report: Iberia Lineas Aereas De Espana (Iberian Airlines) McDonnell Douglas DC-10-30, EC CBN Logan International Airport, Boston, Massachusetts, December 17, 1973. NTSB-AAR-74-14, National Transportation Safety Board, Nov. 8, 1974.

3. Aircraft Accident Report - Eastern Air Lines, Inc., Boeing 727-225 John F. Kennedy International Airport, Jamaica, New York, June 24, 1975. NTSB-AAR-76-8, National Transportation Safety Board, Mar. 12, 1976.

4. Luers, James K.; and Reeves, Jerry B.: Effect of Shear on Aircraft Landing. NASA CR-2287, 1973.

5. Hamel, P.; and Bucholz, F. G.: Gust Effects on the Dynamics of Aircraft During Landing Approach. NASA TT F-12,751, 1970.

6. Working Group of Flight Mechanics Panel: Approach and Landing Simulation. AGARD-R-632, Oct. 1975.

7. Gera, Joseph: The Influence of Vertical Wind Gradients on the Longitudinal Motion of Airplanes. NASA TN D-6430, 1971.

8. Fujita, T. Theodore: Spearhead Echo and Downburst Near the Approach End of a John F. Kennedy Airport Runway, New York City. PB 254009, Nat. Environ. Satellite Service, U.S. Dep. Comm., Mar. 1976.

9. Sherman, Windsor L.; and Winfrey, Sylvia W.: Preliminary Study of a Possible Automatic Landing System. NASA TN D-7611, 1974.

10. Pinsker, W. J. G.: Theoretical Assessment of the General Stability and Gust Response Characteristics of STOL Aircraft. R. & M. No. 3686, Brit. A.R.C., Feb. 1971.

11. Neumark, S.: Problems of Longitudinal Stability Below Minimum Drag Speed and Theory of Stability Under Constraint. R. & M. No. 2983, Brit. A.R.C., 1957.

12. Etkin, Bernard: Dynamics of Atmospheric Flight. John Wiley & Sons, Inc., c.1972.

13. Nicks, Oran W.: A Simple Total Energy Sensor. NASA TM X-73928, 1976.

14. Joppa, Robert G.: Wind Shear Detection Using Measurement of Aircraft Total Energy Change. NASA CR-137839, 1976.

15. Crane, Harold L.; Sommer, Robert W.; and Healy, Frederick M.: Effects of Reduced Airspeed for Landing Approach on Flying Qualities of a Large Jet Transport Equipped With Powered Lift. NASA TN D-4804, 1968.

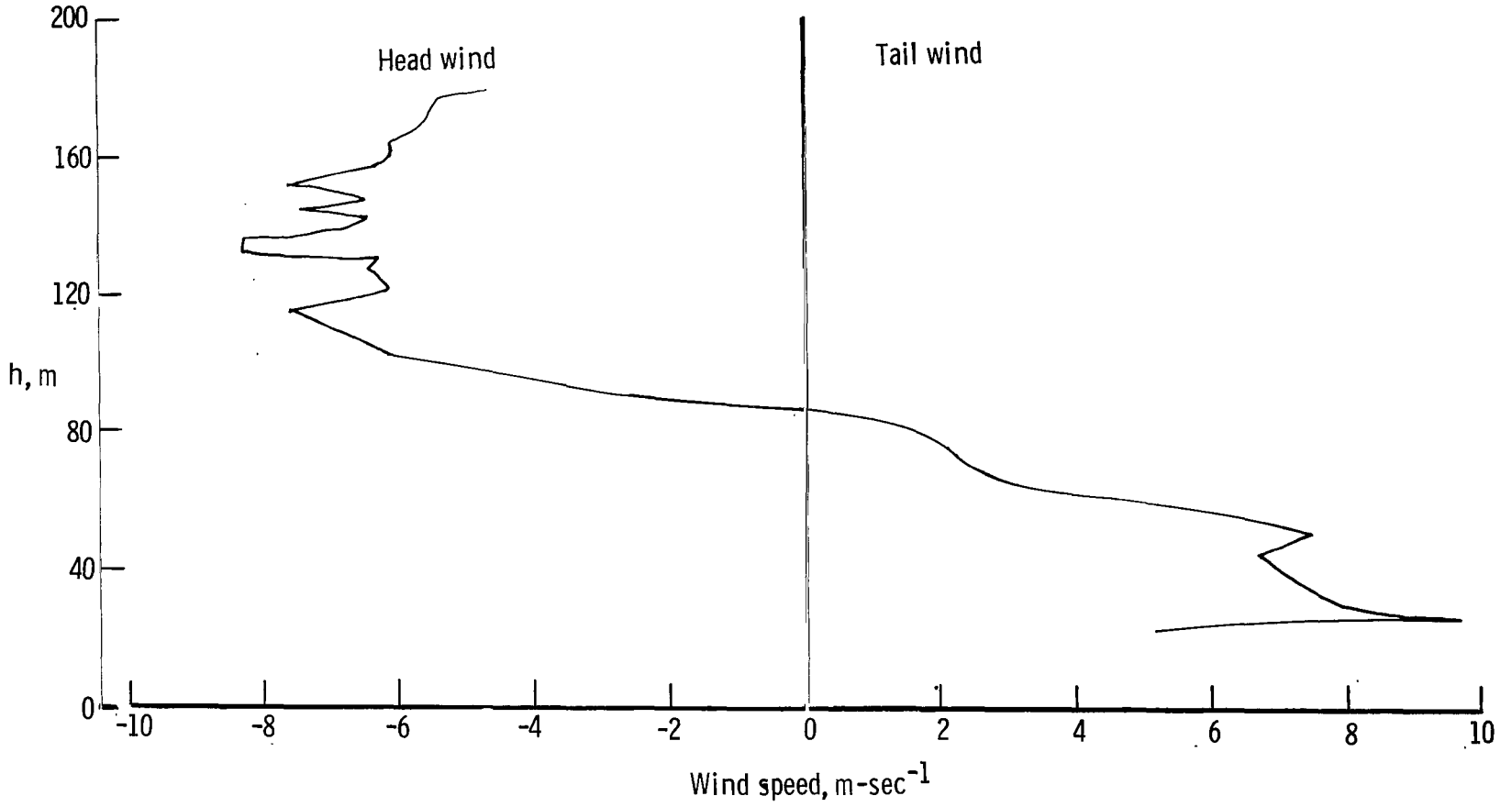

Figure 1.- Variation of wind speed with altitude for a strong wind shear. Head winds are negative.

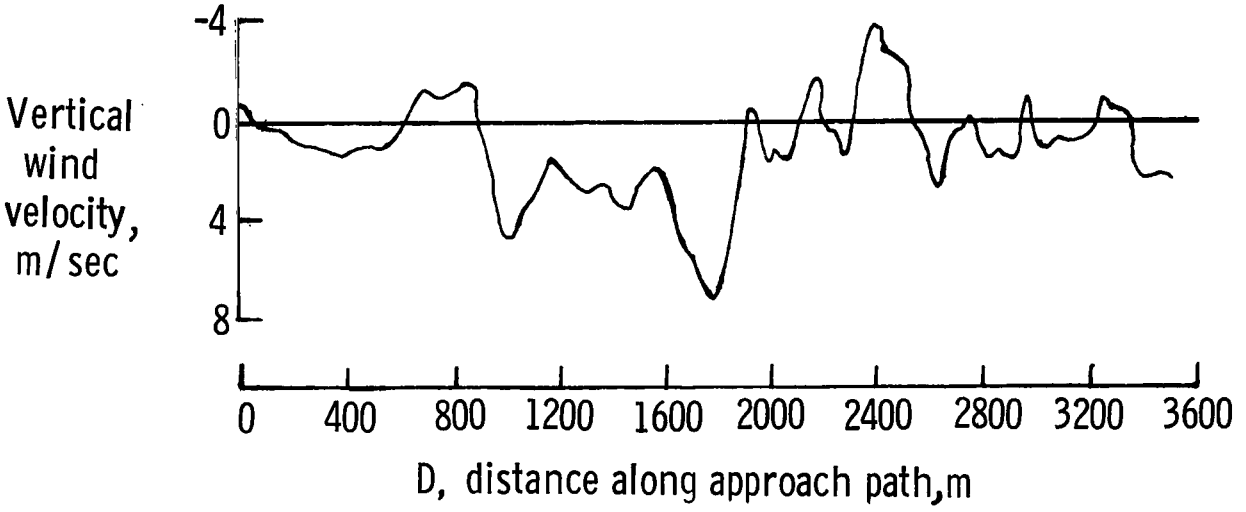

Figure 2.- Updrafts and downdrafts that co-existed with the vertical shear shown in figure 1.

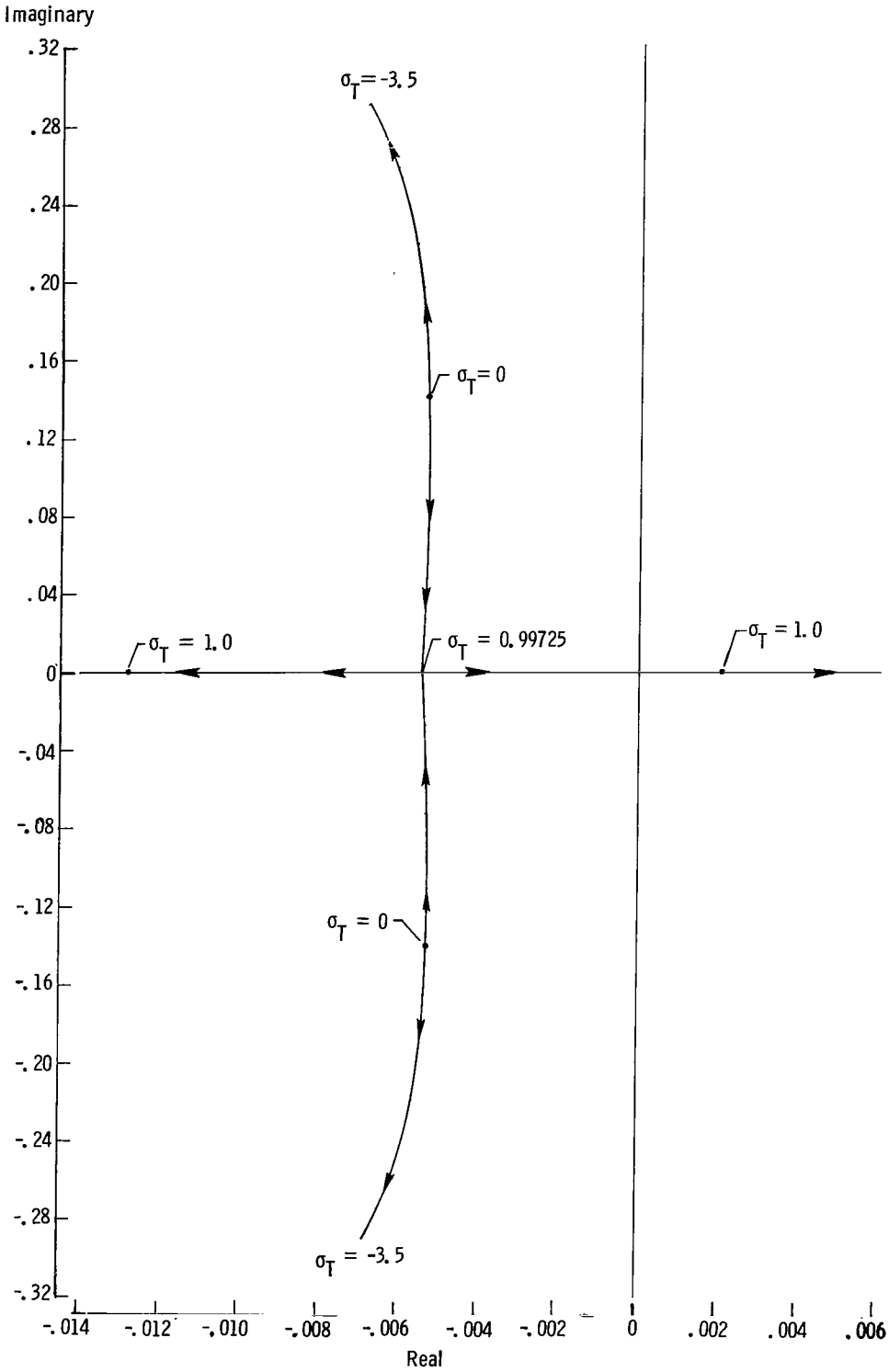

Figure 3.- Root-locus plot for the phugoid mode Γ_0 = -0.05236 radian; σ_w = 0; σ_T = σ_u.

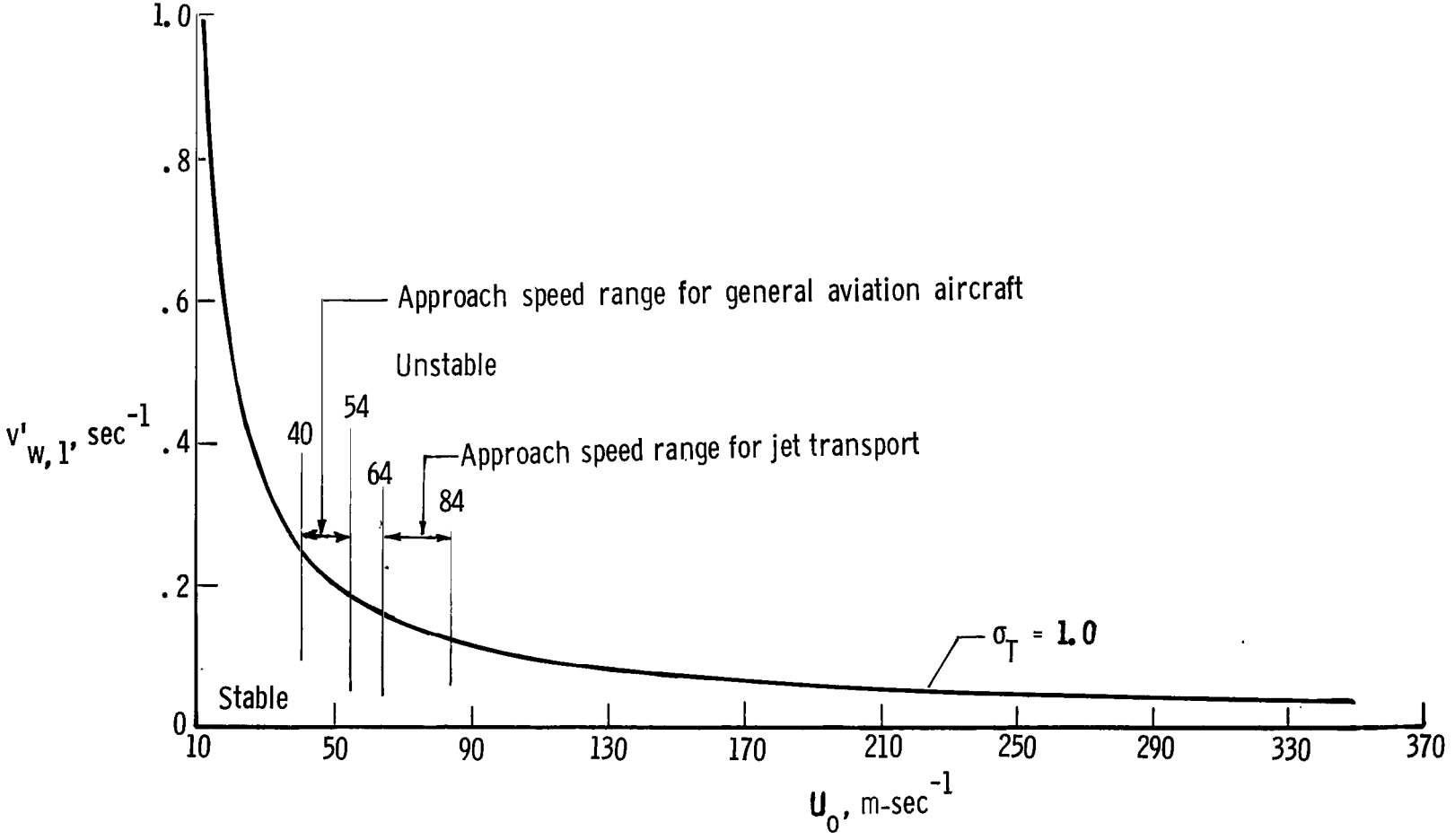

(a) Boundary for all aircraft.

Figure 4.- Phugoid stability boundary for positive vertical wind shear.
$\sigma_T = \sigma_u$; $\sigma_w = 0$.

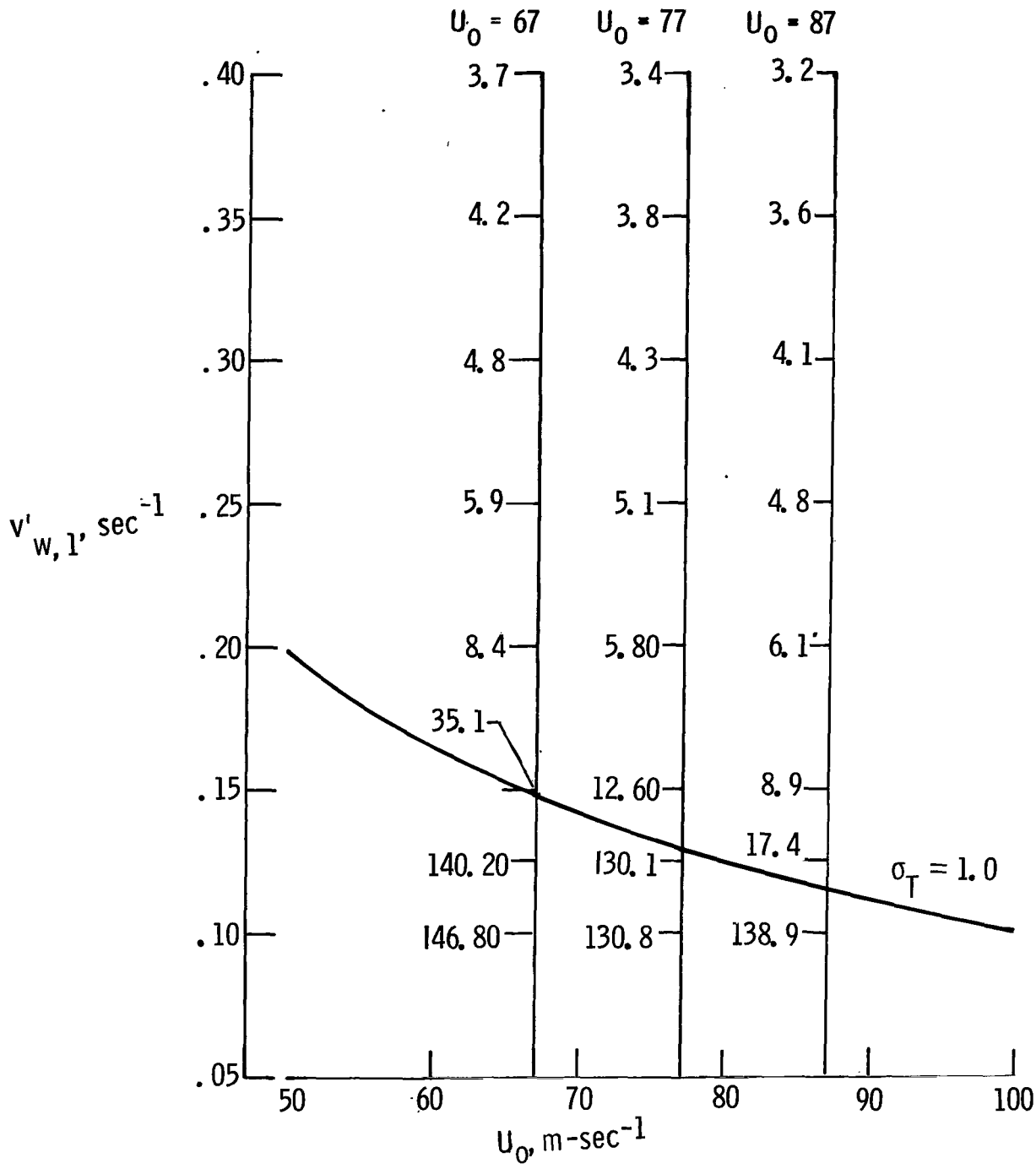

(b) Effect of changing approach speed on the phugoid stability. The numbers below curve are times to damp to half amplitude, and those above are time to double amplitude.

Figure 4.- Concluded.

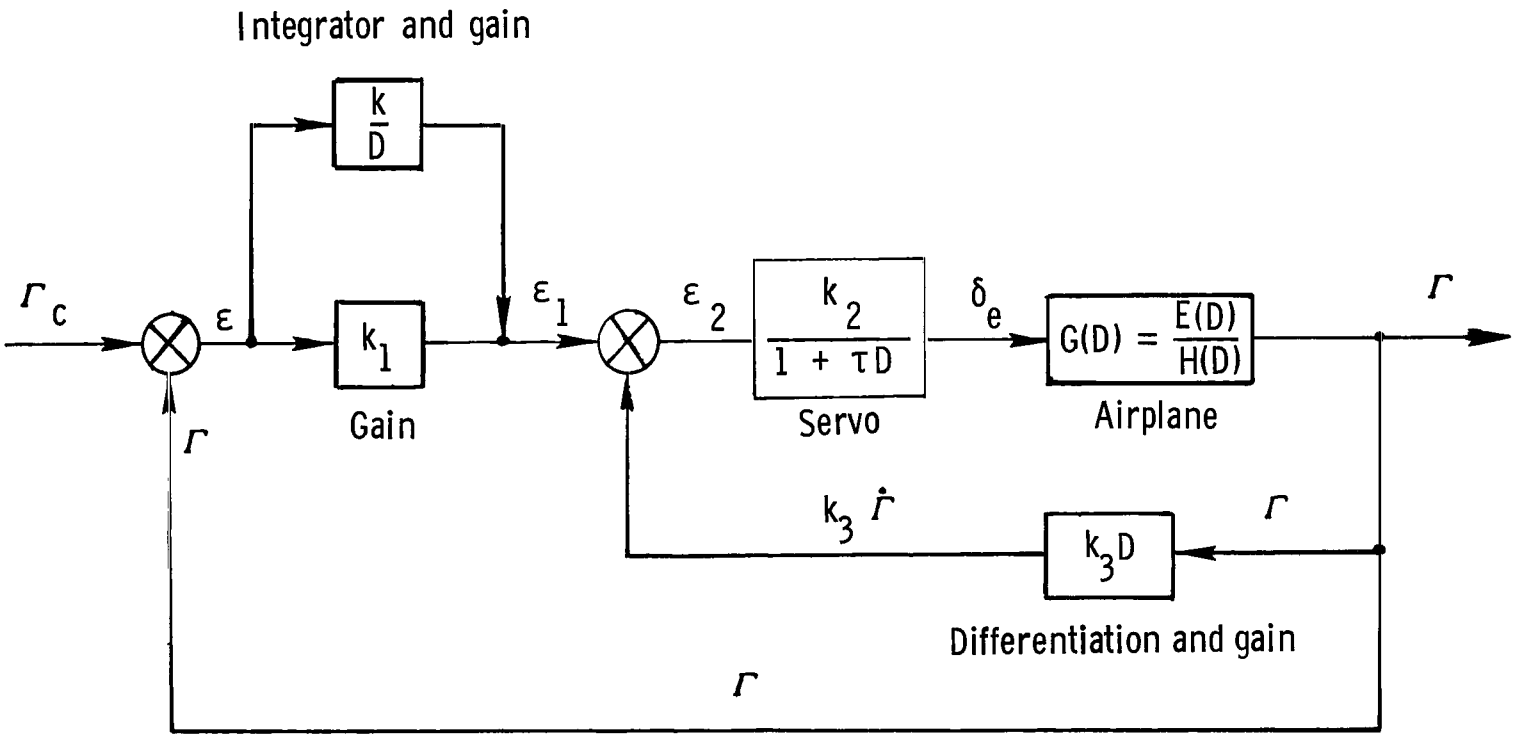

$$\varepsilon = \Gamma_c - \Gamma \; ; \; \varepsilon_1 = k_1 \varepsilon + \frac{k\varepsilon}{D} ; \; \varepsilon_2 = \varepsilon_1 - k_3 D \Gamma$$

Figure 5.- Block diagram of automatic pilot used in stability studies.

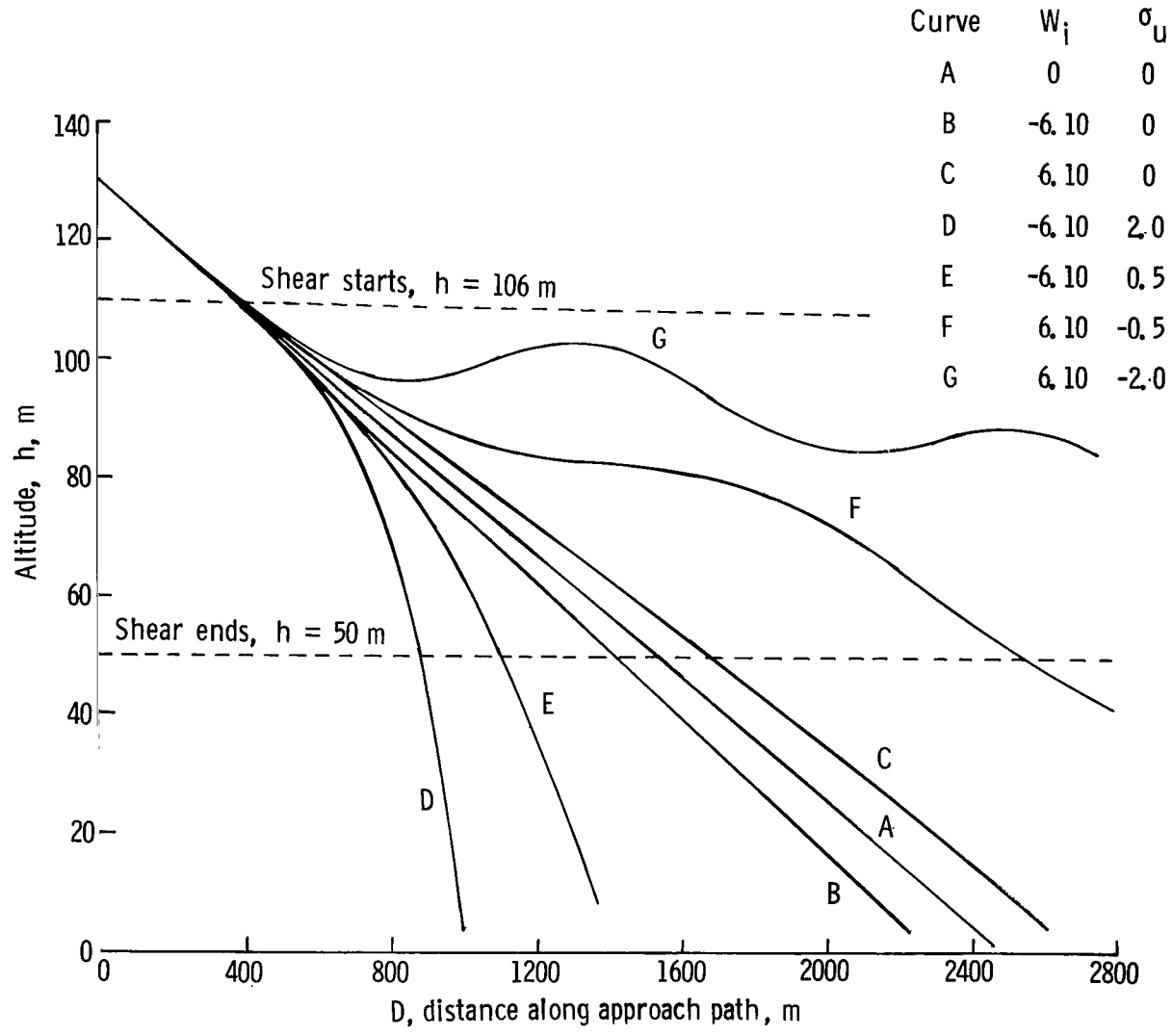

(a) Altitude.

Figure 6.- Control-fixed motion of an airplane in wind shear. $\sigma_T = \sigma_u$; $\sigma_w = 0$.

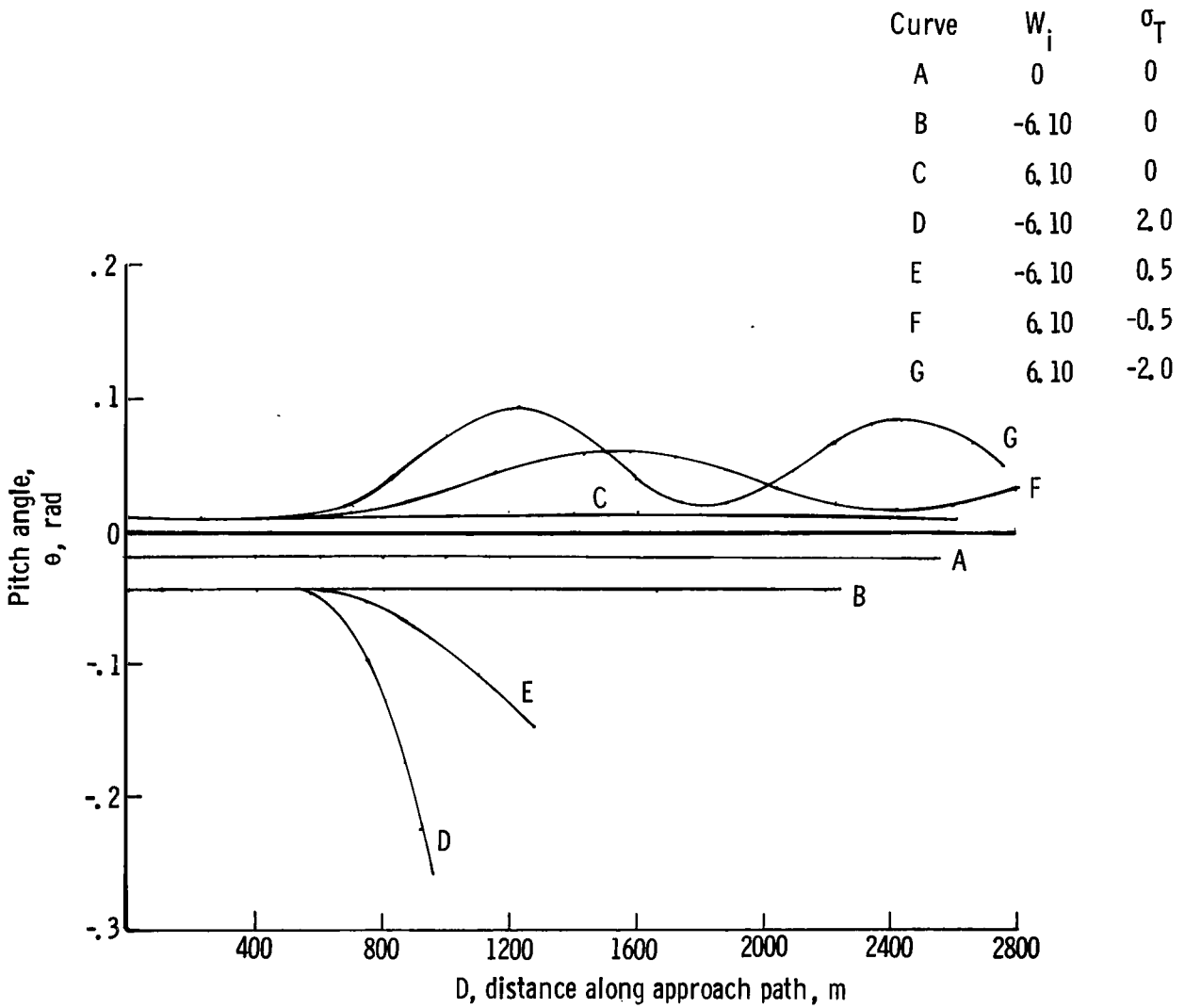

(b) Pitch angle.

Figure 6.- Continued.

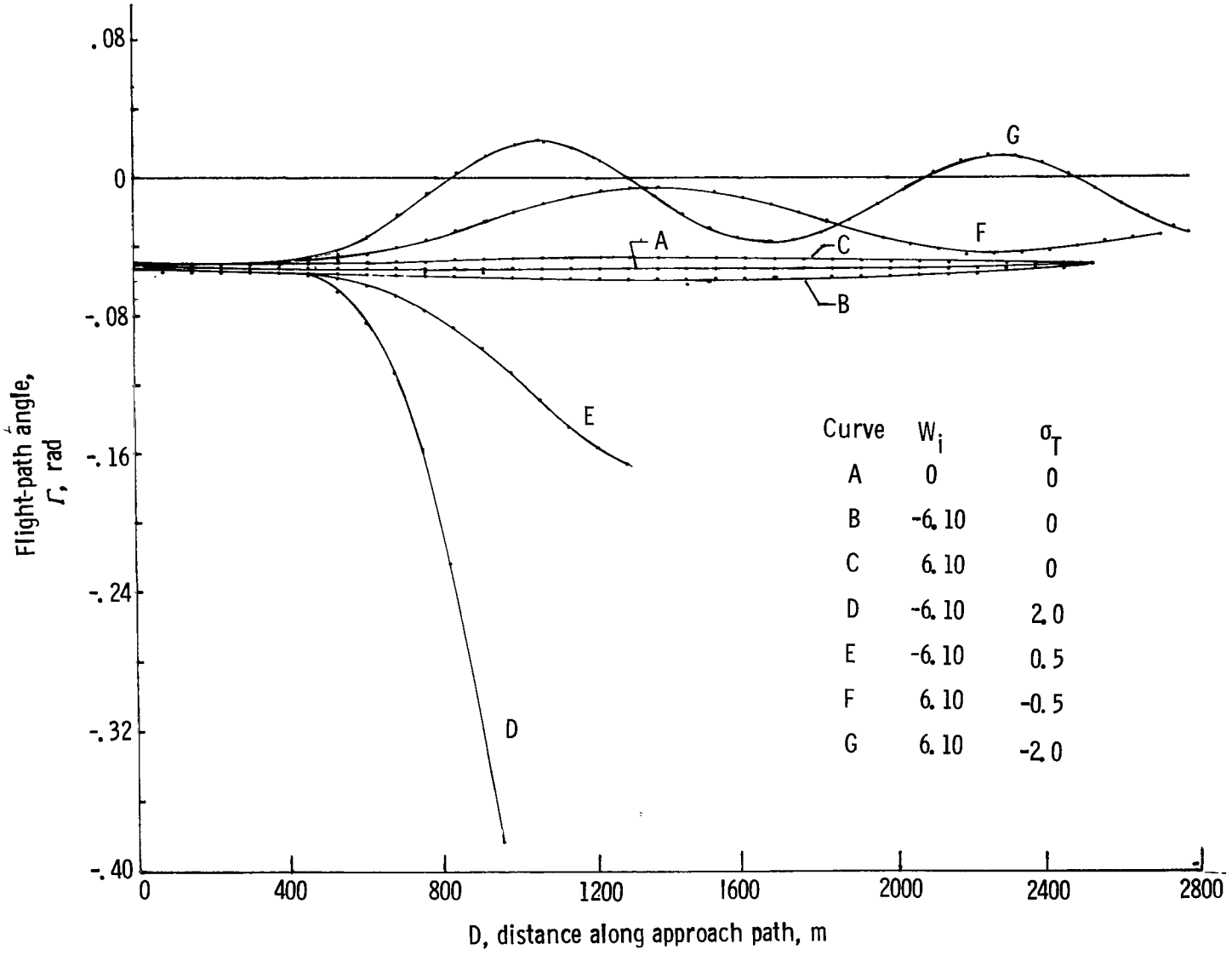

(c) Flight-path angle.

Figure 6.- Concluded.

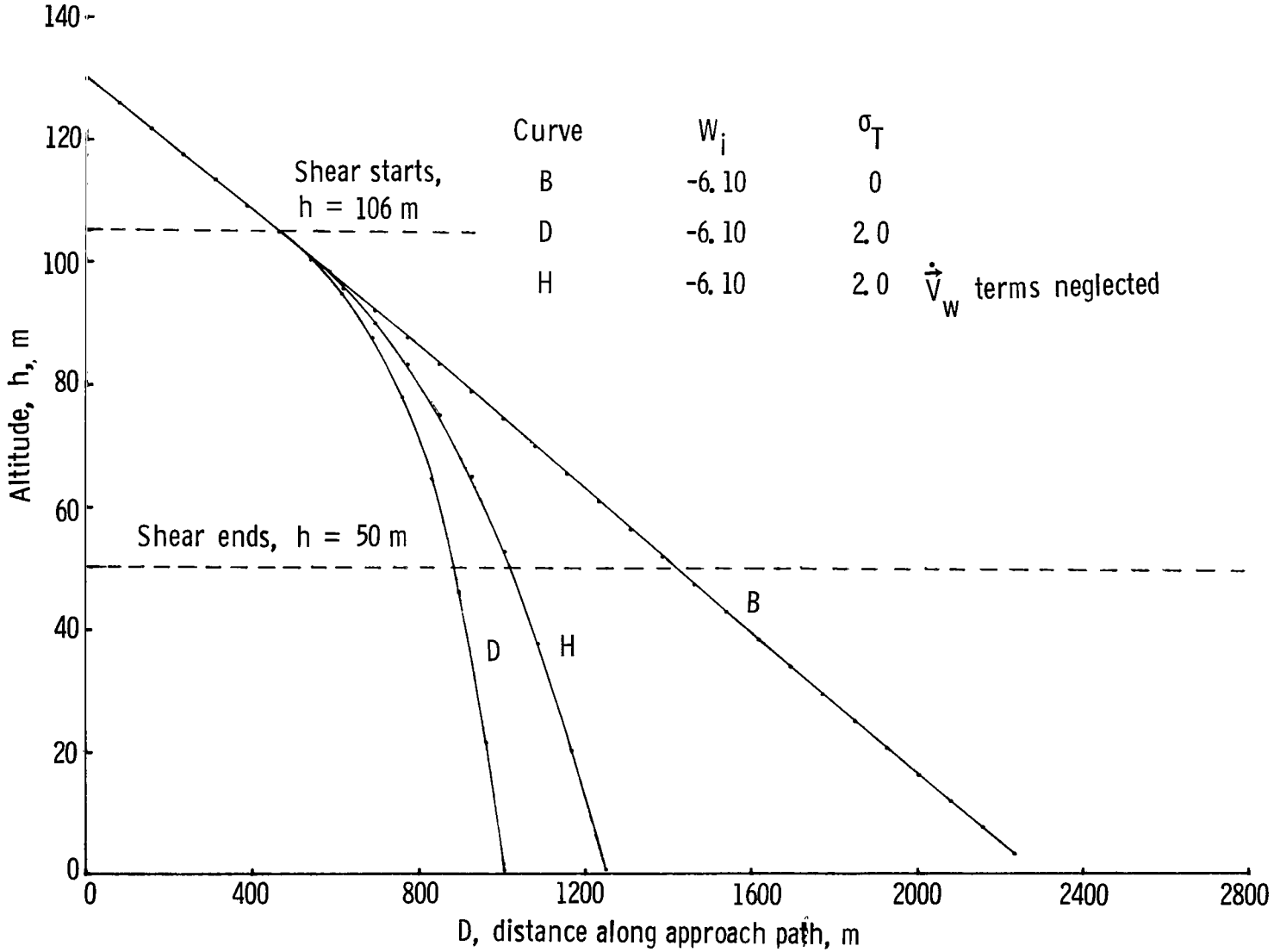

(a) Altitude.

Figure 7.- The effect of deleting wind acceleration terms in the kinematics of the airplane equations when the wind shear is positive. $\sigma_T = \sigma_u$; $\sigma_w = 0$. Motions are control fixed.

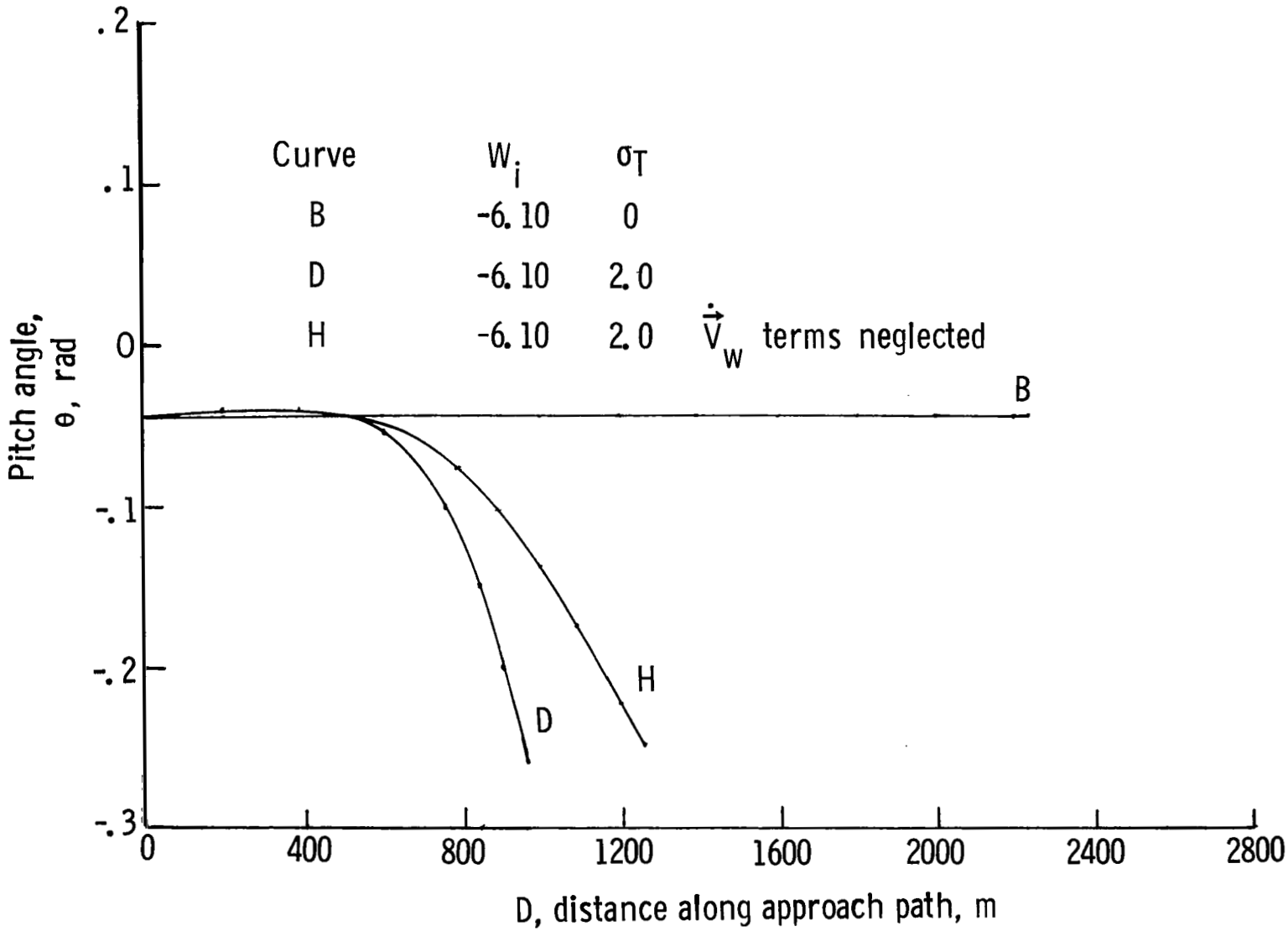

(b) Pitch angle.

Figure 7.- Continued.

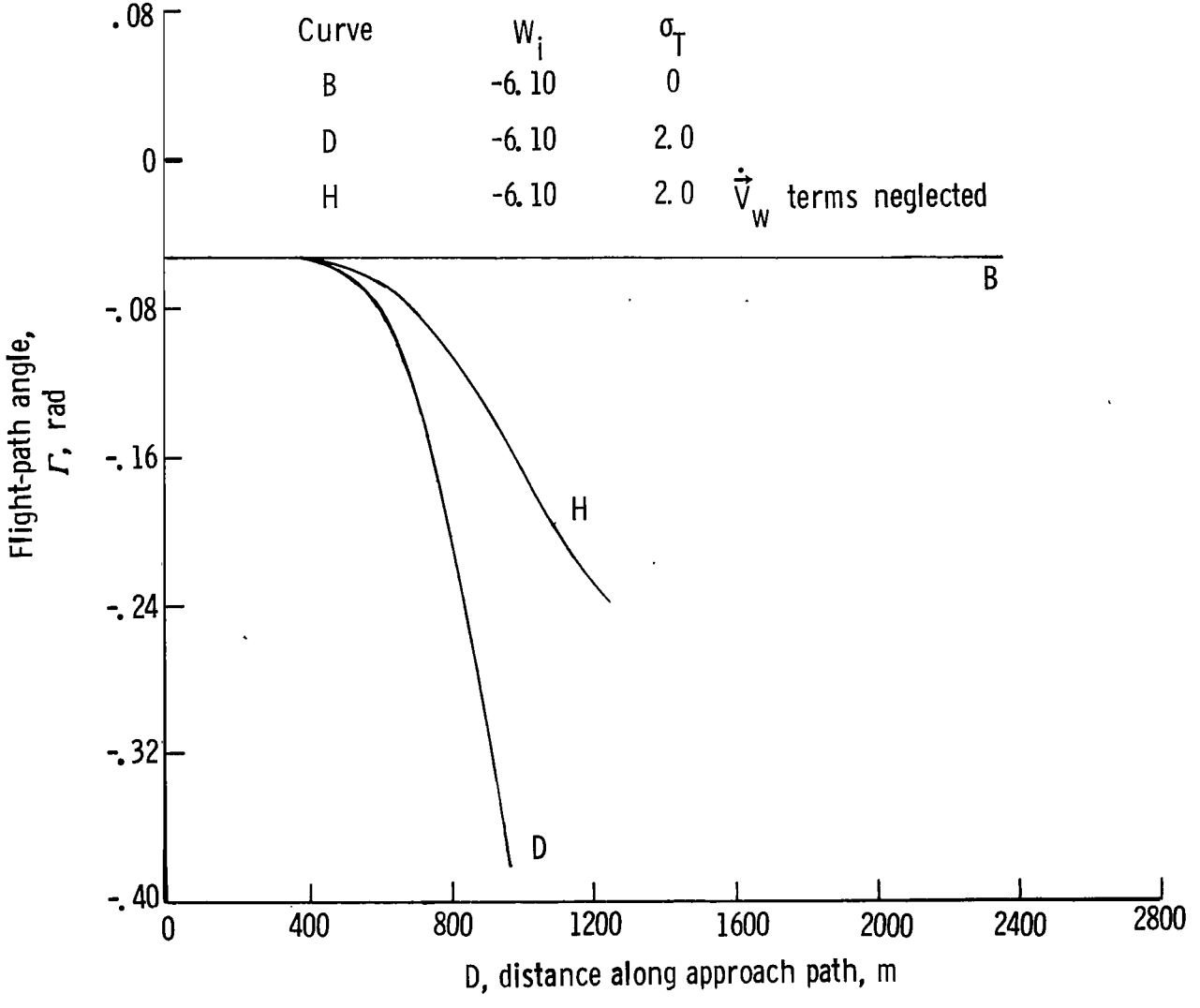

(c) Flight-path angle.

Figure 7.- Concluded.

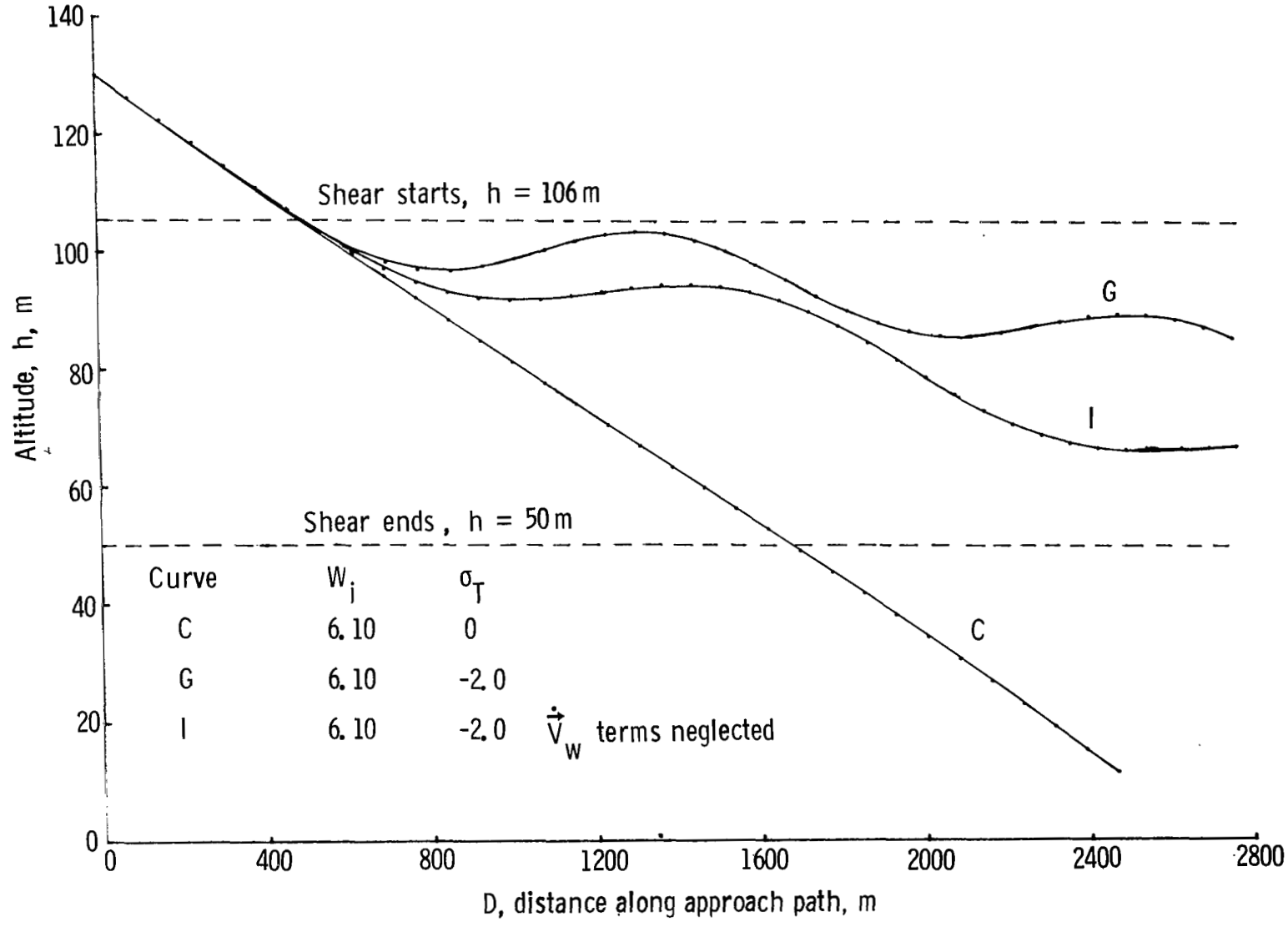

(a) Altitude.

Figure 8.- The effect of deleting wind acceleration terms in the kinematics of the airplane equations of motion when the wind shear is negative. $\sigma_T = \sigma_u$; $\sigma_w = 0$. Motions are control fixed.

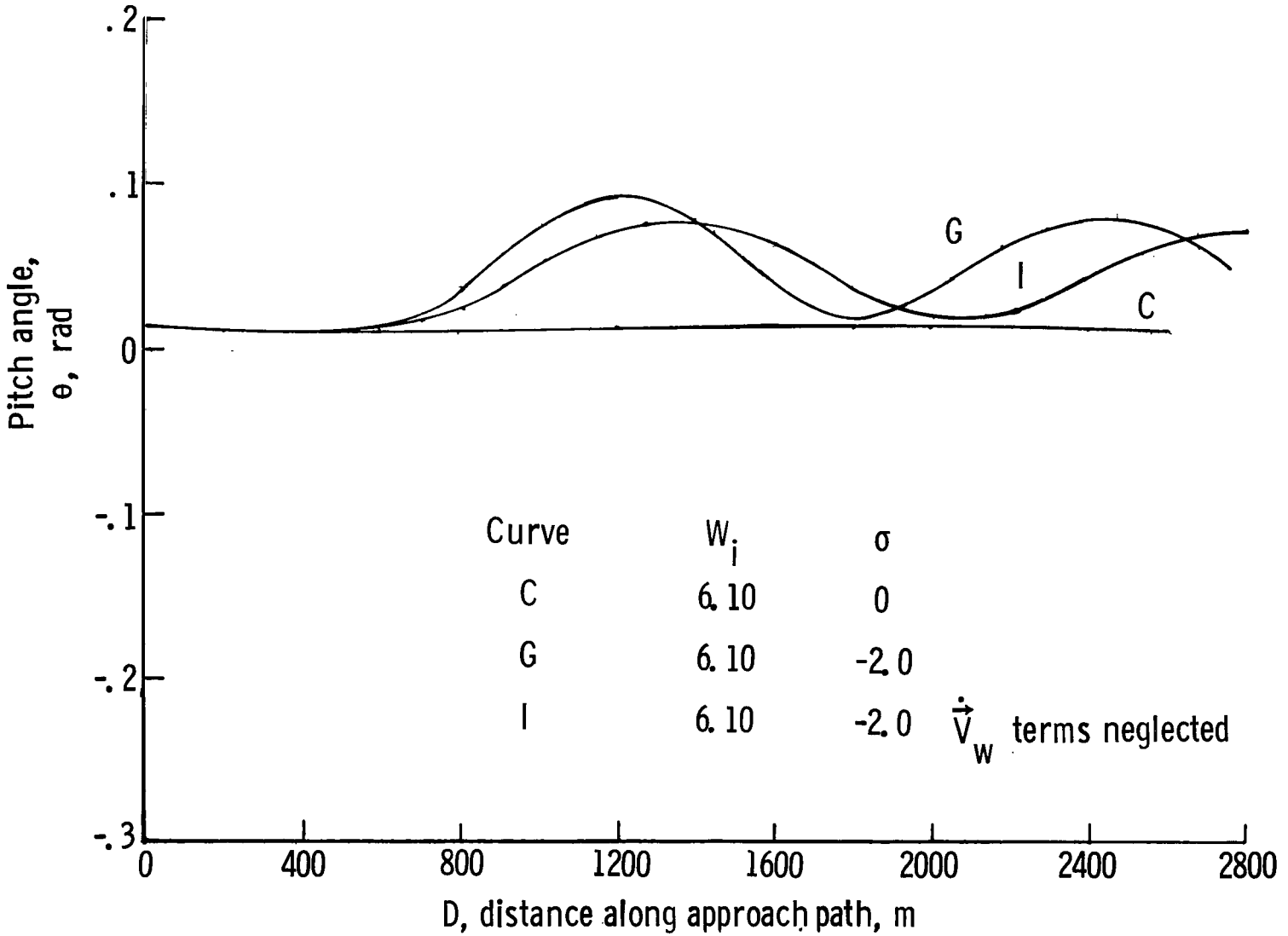

(b) Pitch angle.

Figure 8.- Continued.

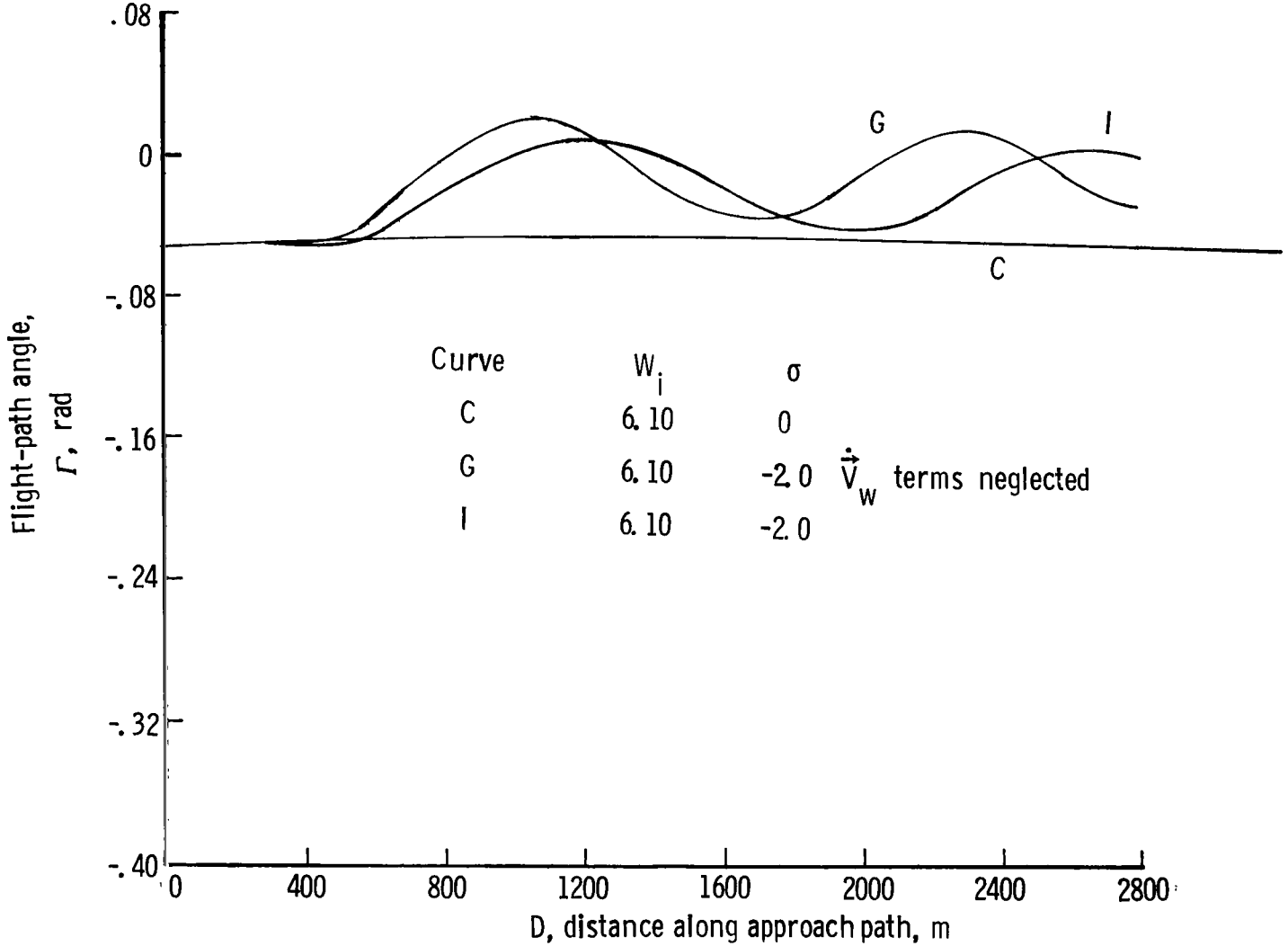

(c) Flight-path angle.

Figure 8.- Concluded.

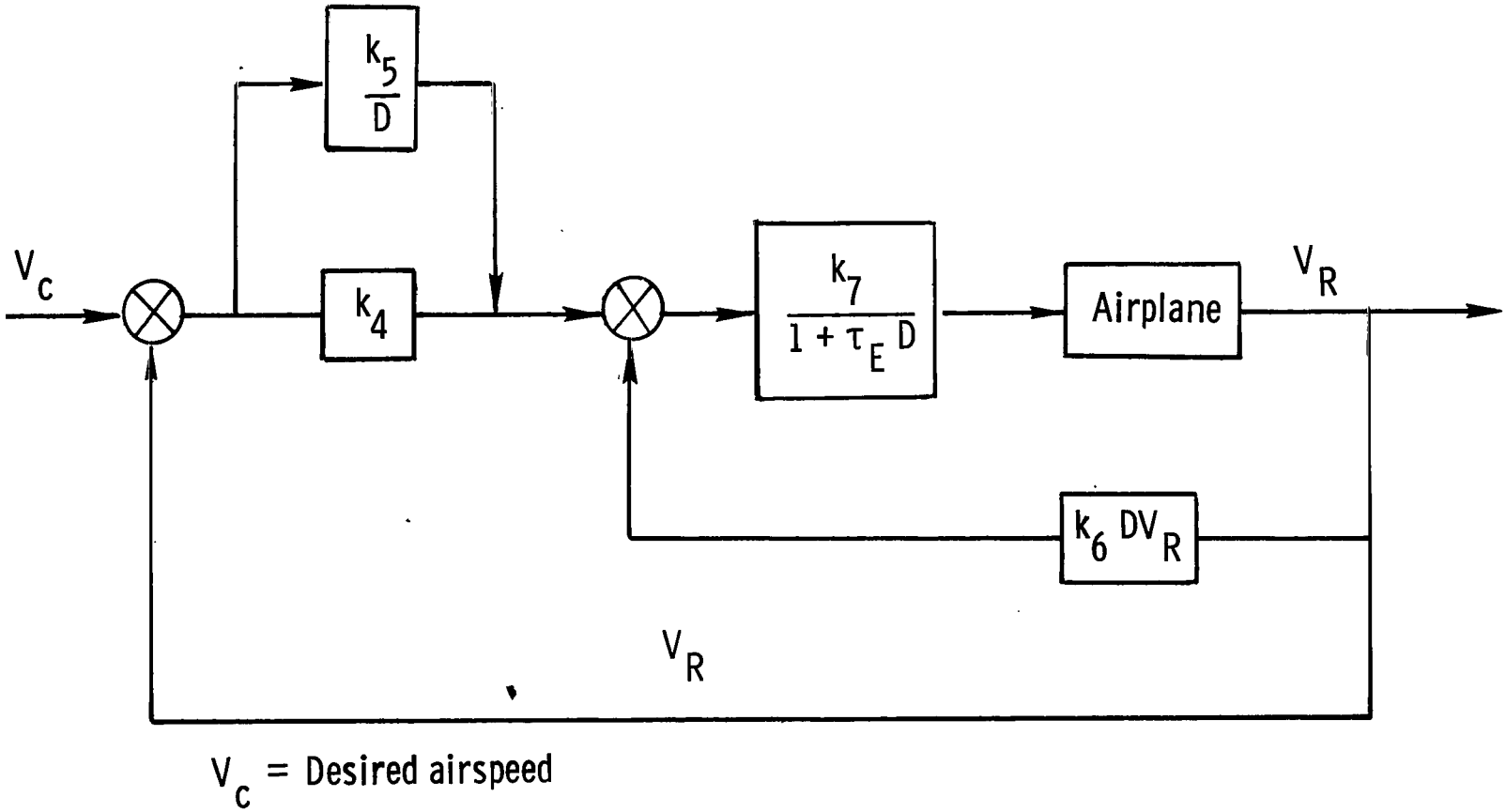

Figure 9.- Block diagram of speed control system.

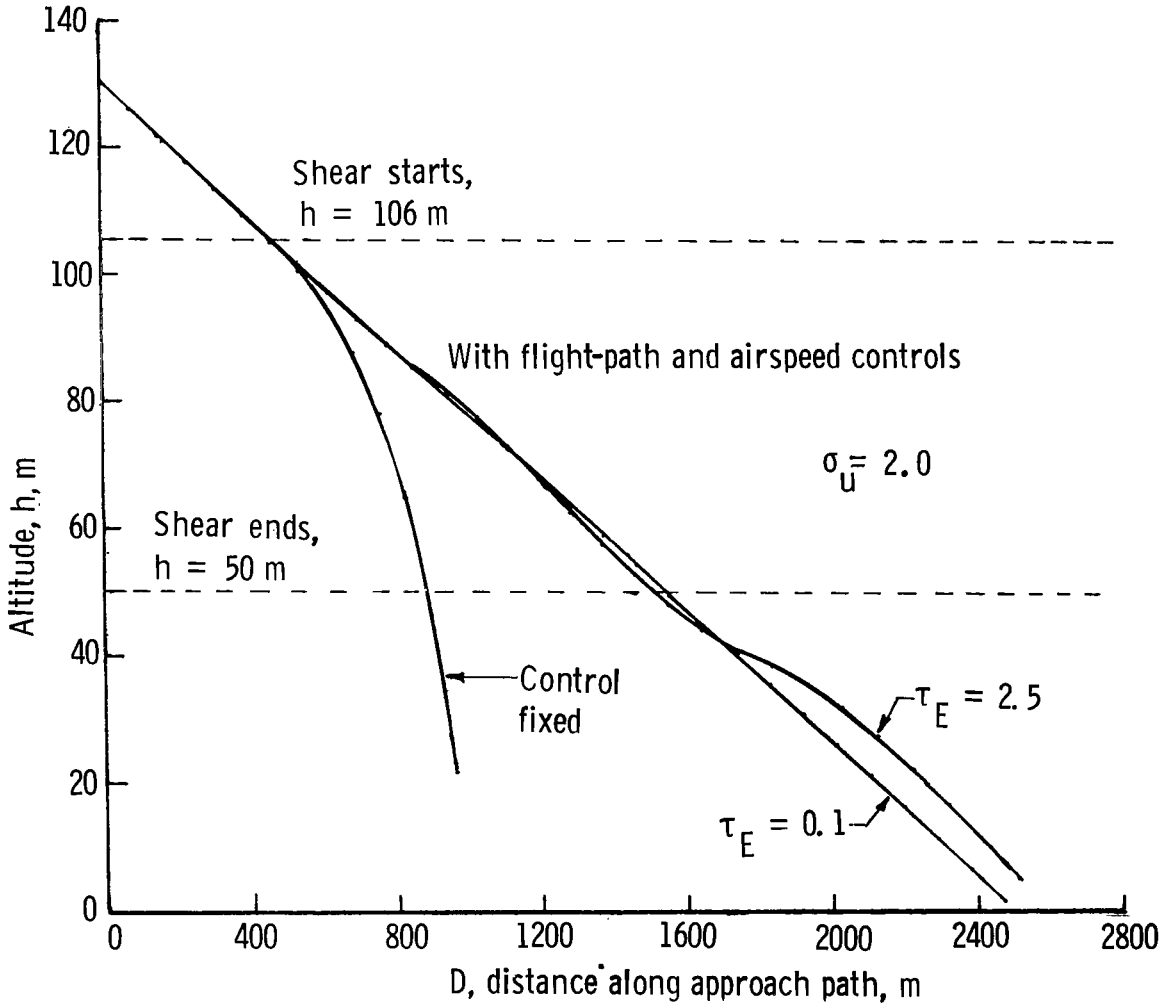

(a) Altitude.

Figure 10.- Comparison of airplane motions in positive wind shear. $\sigma_T = \sigma_u = 2.0$, with and without automatic flight-path and speed controls.

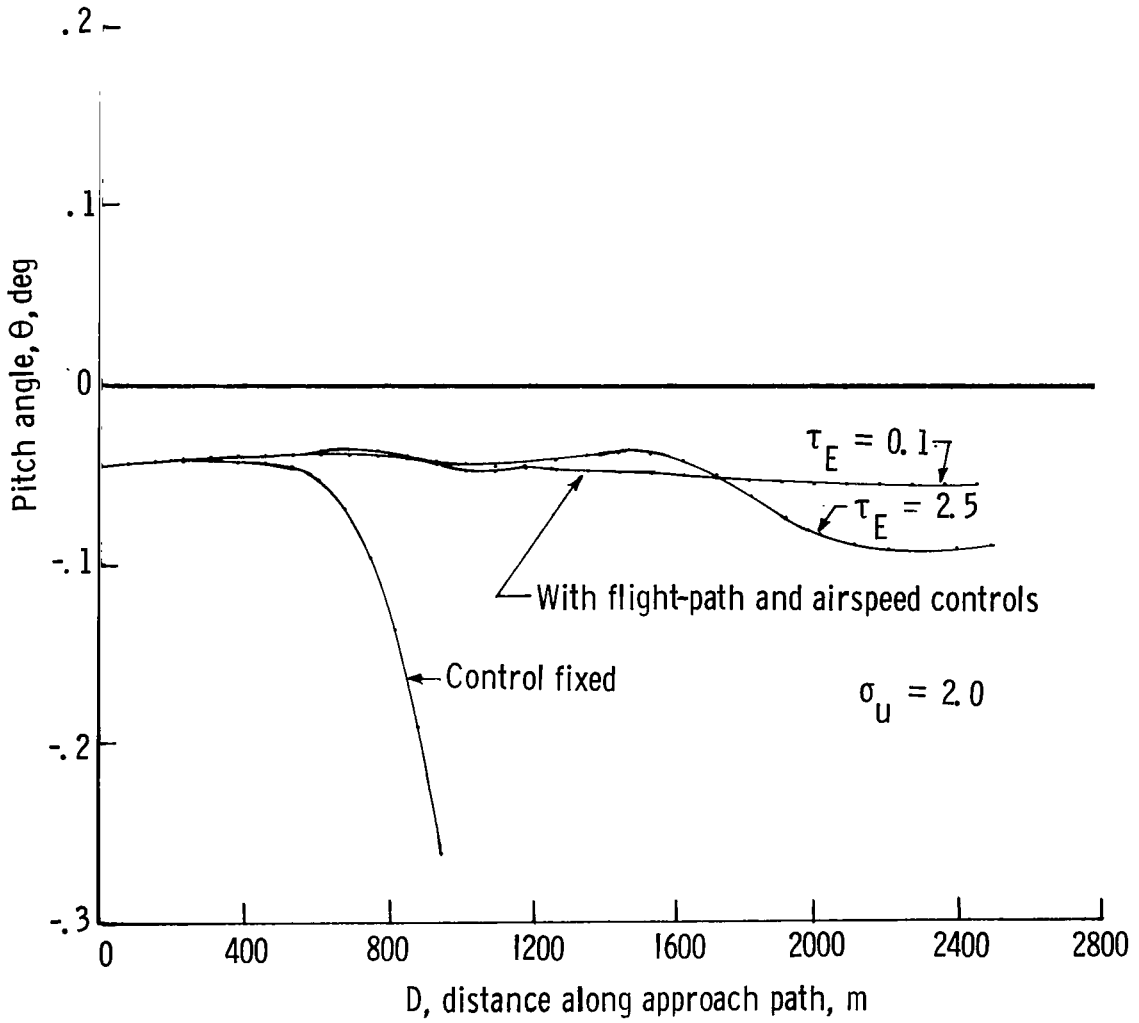

(b) Pitch angle.

Figure 10.- Continued.

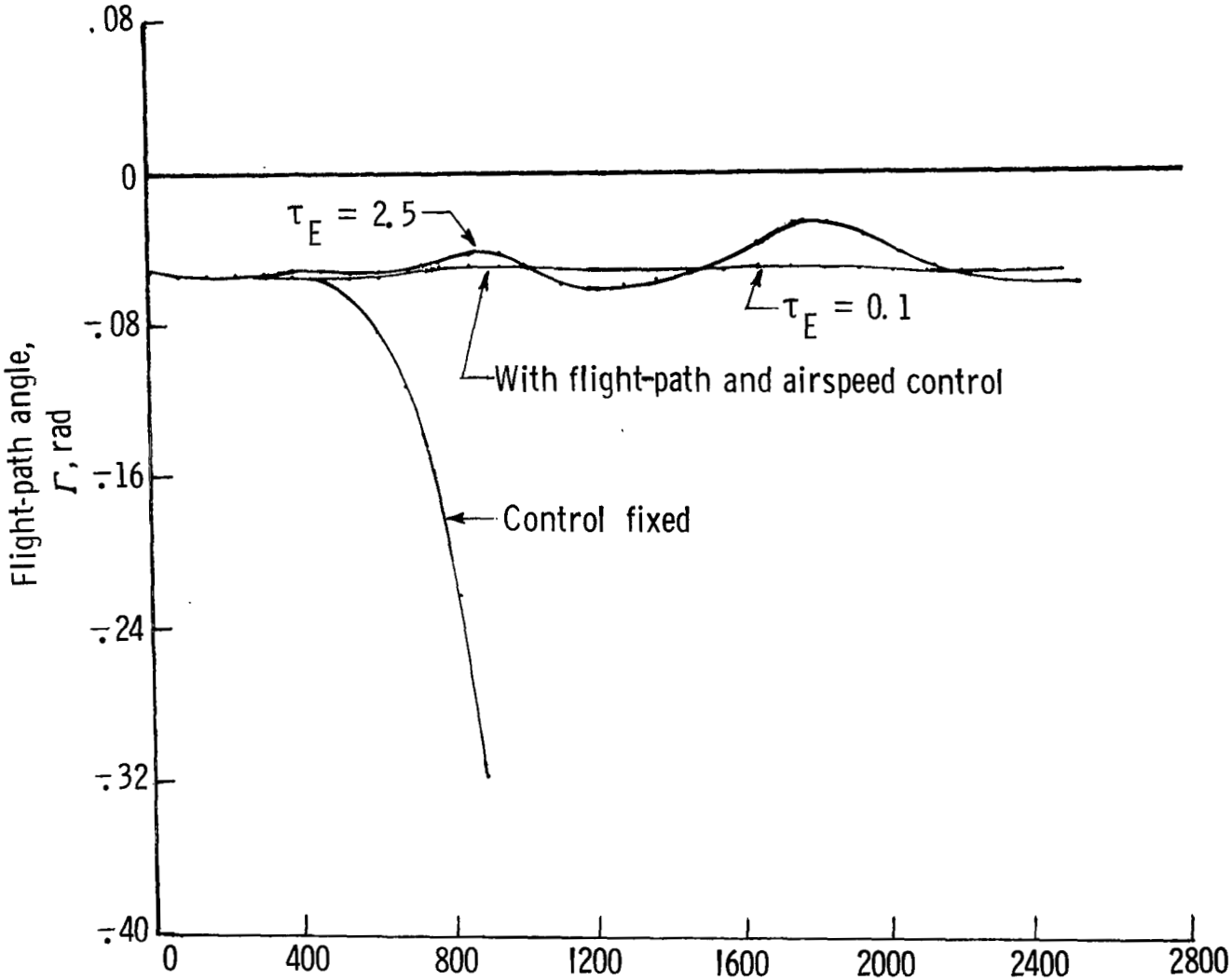

(c) Flight-path angle.

Figure 10.- Concluded.

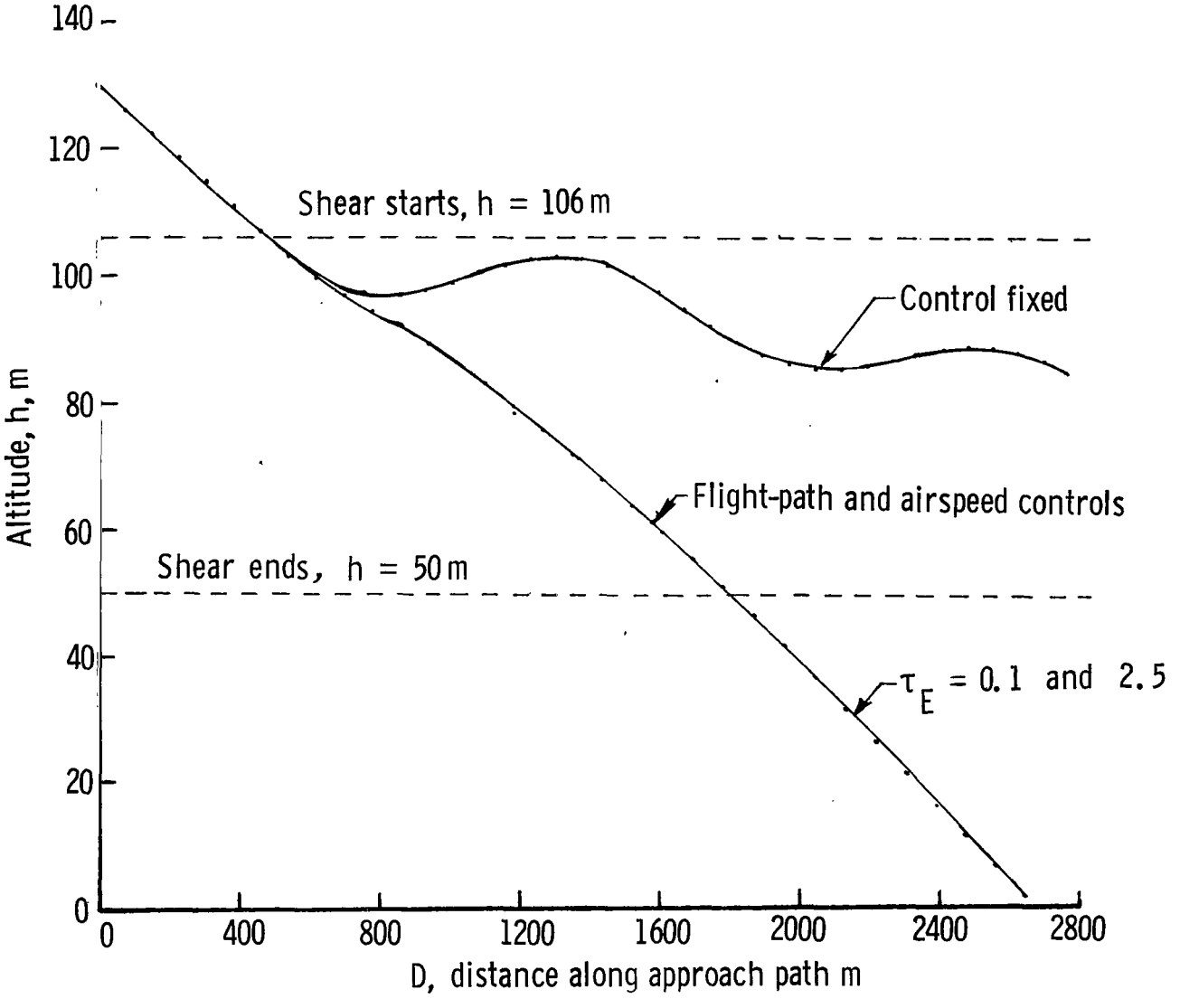

(a) Altitude.

Figure 11.- Comparison of airplane motions in negative wind shear. $\sigma_T = \sigma_u$ = -2.0, with and without automatic flight-path and speed controls. $\sigma_w = 0$.

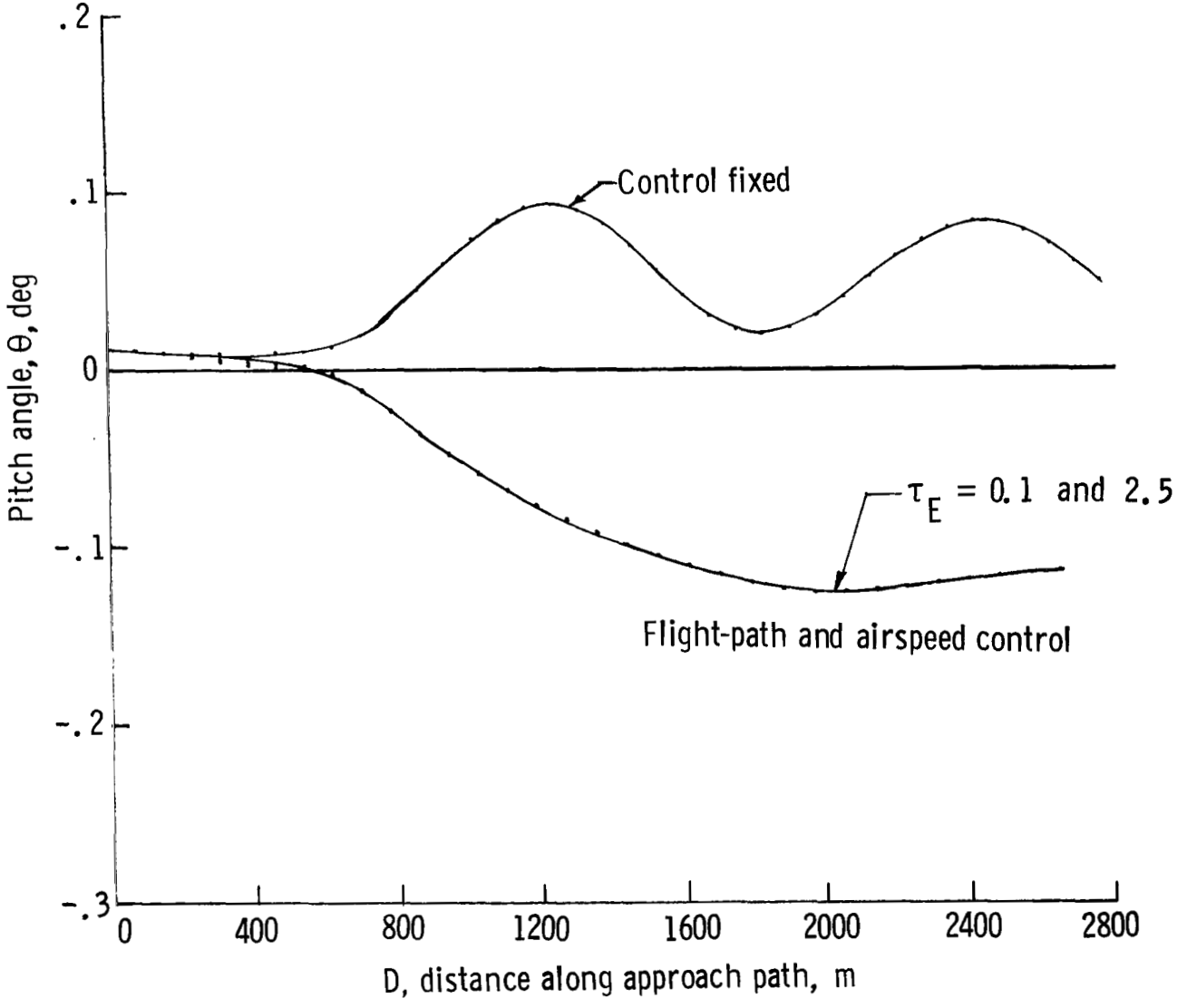

(b) Pitch angle.

Figure 11.- Continued.

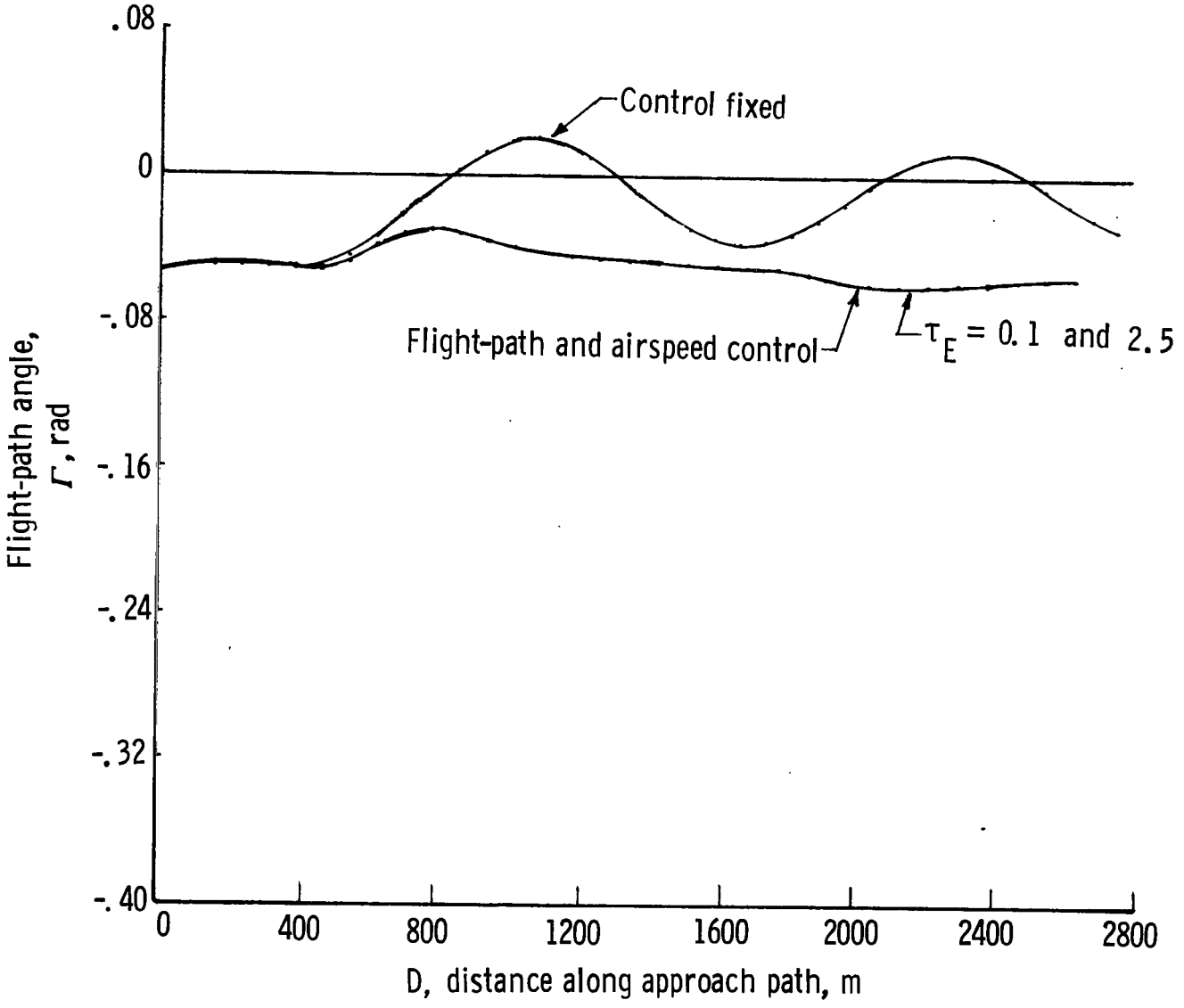

(c) Flight-path angle.

Figure 11.- Concluded.

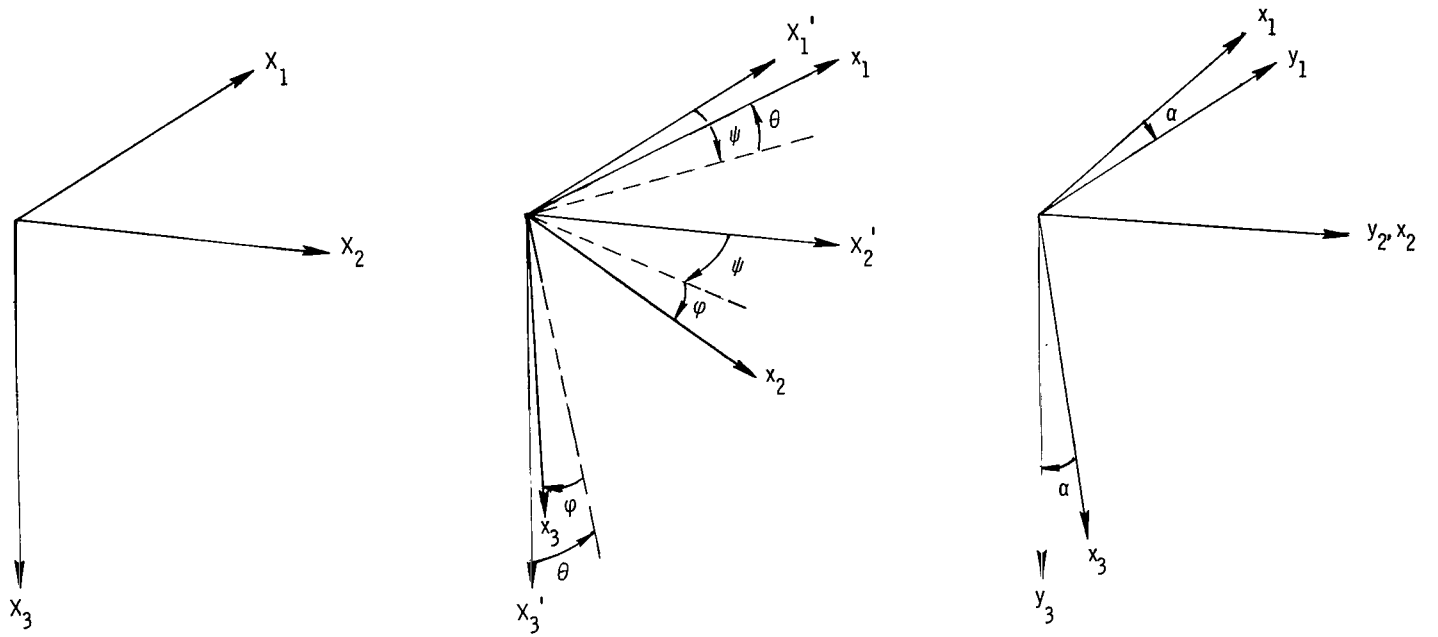

Earth-fixed axes, X_1, X_2, X_3

Moving axes, X_1', X_2', X_3' and principal body axes, x_1, x_2, x_3

Intermediate axes are not labeled and are shown as dashed lines

Stability axes, y_1, y_2, y_3 and principal body axes, x_1, x_2, x_3

Figure 12.- Coordinate systems and Euler angles. The order of rotation for the Euler angles is ψ, θ, and φ. The moving axes translate with airplane and remain parallel to the earth-fixed axes. Positive directions are shown.

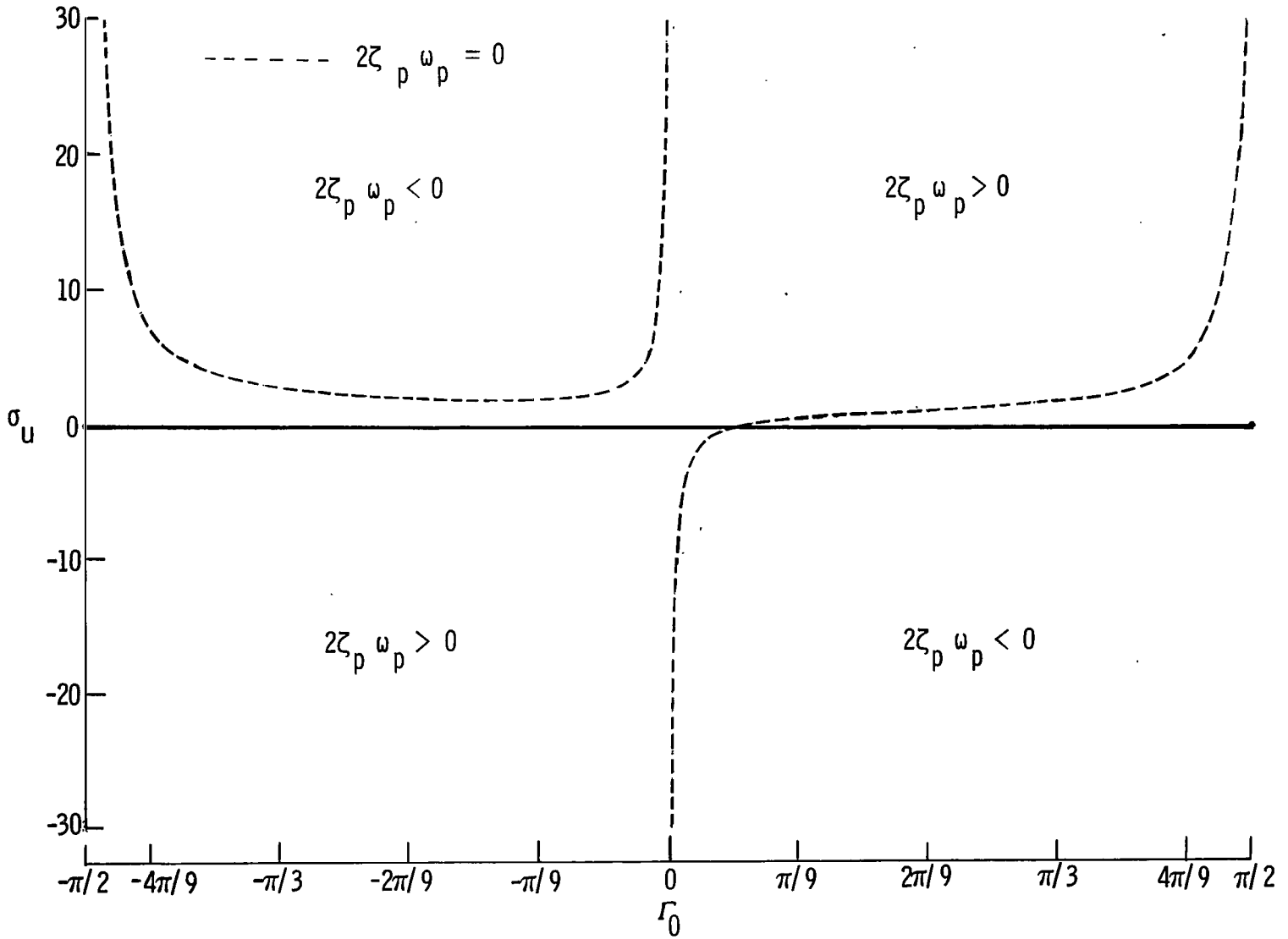

Figure 13.- Combinations of Γ_0 and σ_u that make the $2\zeta_p\omega_p$ term of equation (C5) zero.

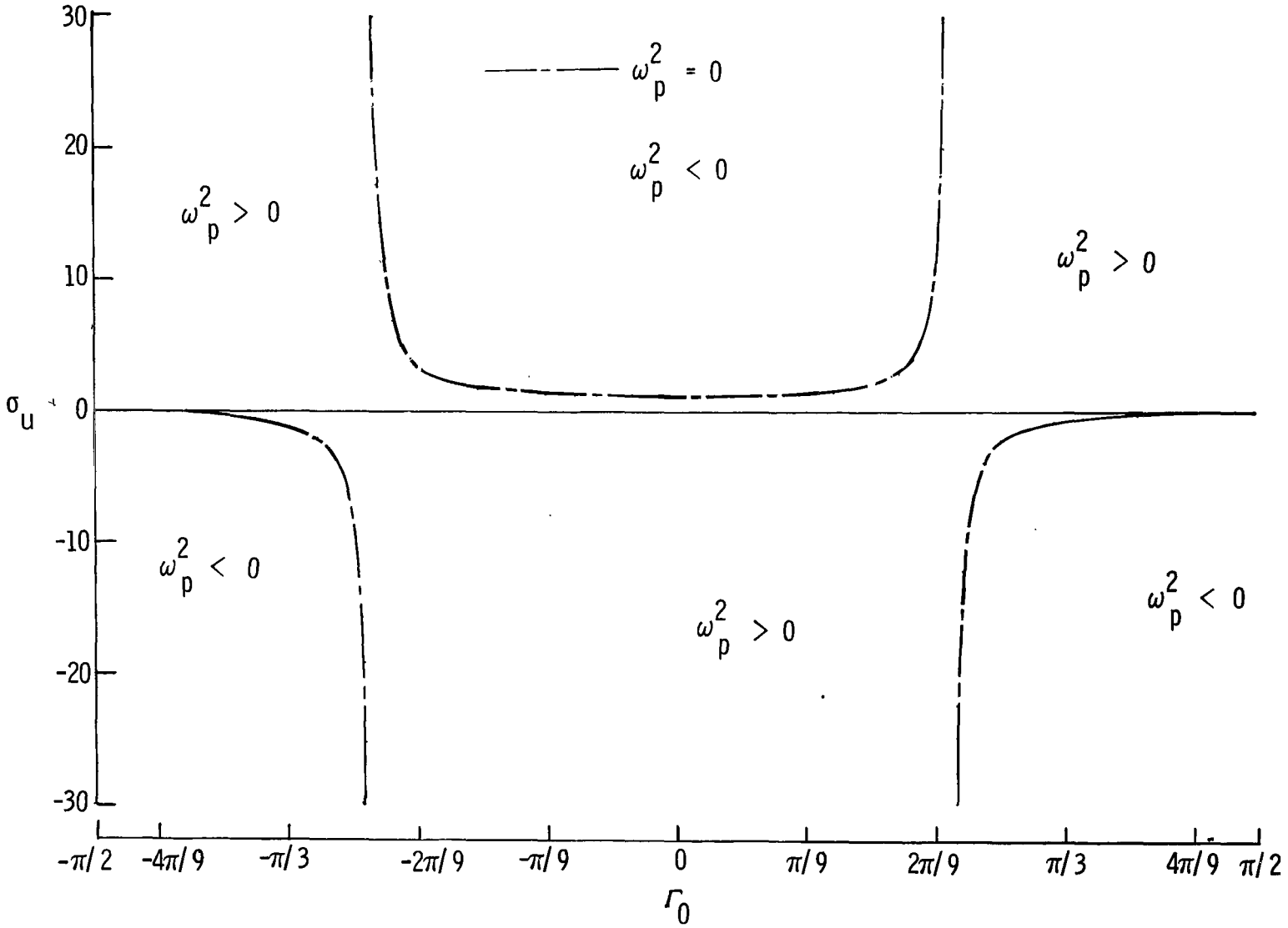

Figure 14.- Combinations of Γ_0 and σ_u that make the term ω_p^2 of equation (C6) zero.

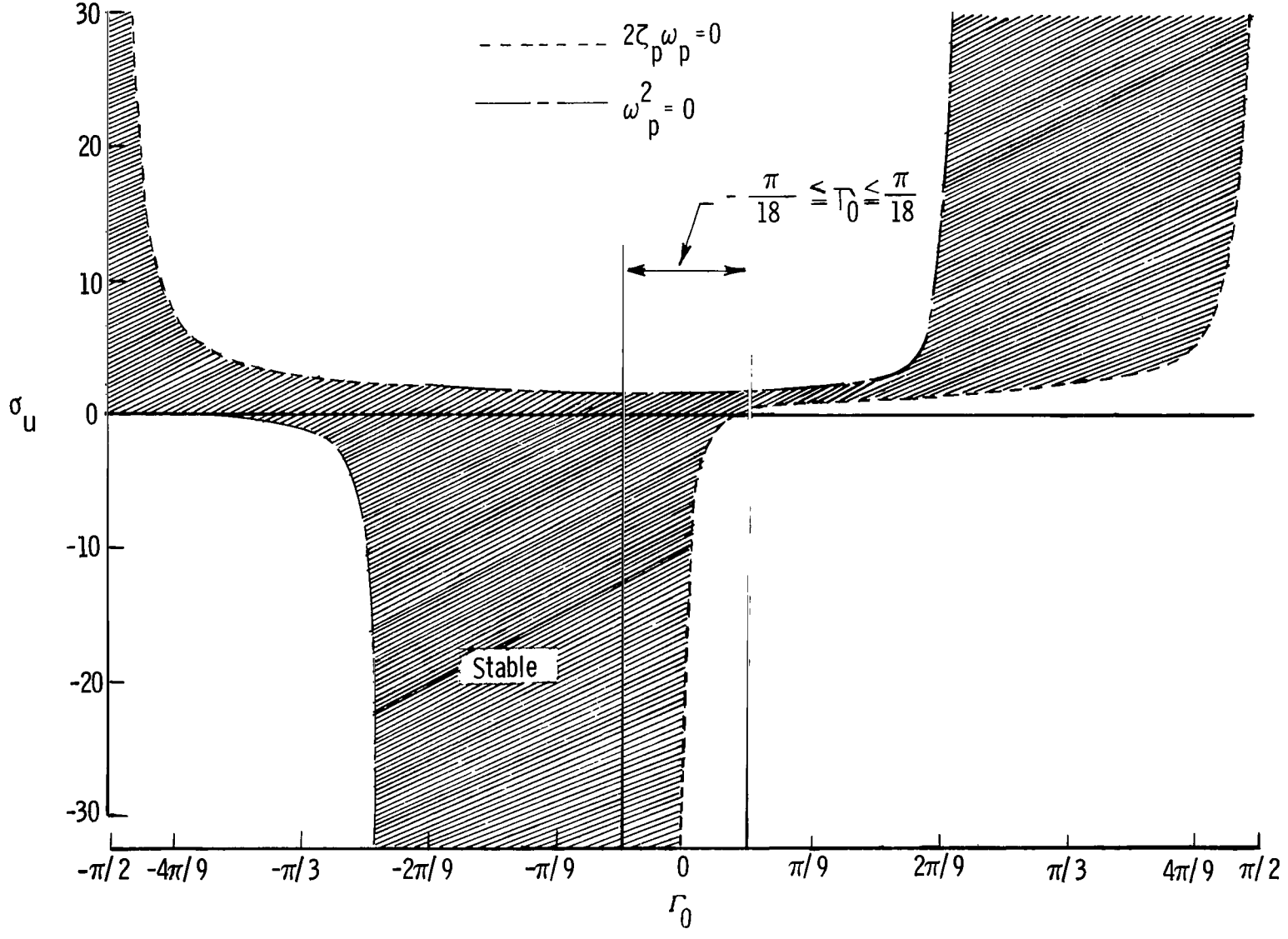

Figure 15.- Regions of stability for equation (C2) obtained by combining figures 13 and 14.

"The aeronautical and space activities of the United States shall be conducted so as to contribute . . . to the expansion of human knowledge of phenomena in the atmosphere and space. The Administration shall provide for the widest practicable and appropriate dissemination of information concerning its activities and the results thereof."

—NATIONAL AERONAUTICS AND SPACE ACT OF 1958

NASA SCIENTIFIC AND TECHNICAL PUBLICATIONS

TECHNICAL REPORTS: Scientific and technical information considered important, complete, and a lasting contribution to existing knowledge.

TECHNICAL NOTES: Information less broad in scope but nevertheless of importance as a contribution to existing knowledge.

TECHNICAL MEMORANDUMS: Information receiving limited distribution because of preliminary data, security classification, or other reasons. Also includes conference proceedings with either limited or unlimited distribution.

CONTRACTOR REPORTS: Scientific and technical information generated under a NASA contract or grant and considered an important contribution to existing knowledge.

TECHNICAL TRANSLATIONS: Information published in a foreign language considered to merit NASA distribution in English.

SPECIAL PUBLICATIONS: Information derived from or of value to NASA activities. Publications include final reports of major projects, monographs, data compilations, handbooks, sourcebooks, and special bibliographies.

TECHNOLOGY UTILIZATION PUBLICATIONS: Information on technology used by NASA that may be of particular interest in commercial and other non-aerospace applications. Publications include Tech Briefs, Technology Utilization Reports and Technology Surveys.

Details on the availability of these publications may be obtained from:

SCIENTIFIC AND TECHNICAL INFORMATION OFFICE

NATIONAL AERONAUTICS AND SPACE ADMINISTRATION

Washington, D.C. 20546